ACS OMEGA

Open Access

http://pubs.acs.org/journal/acsodf

Article

The Influencing Factors and Mechanism of Anionic and Zwitterionic Surfactant on Viscosity Reduction in Heavy O/W Emulsions

Jiaqiang Jing, Yuting Shan,* Ning Wang, Jie Sun, Cancan Jiang, Lei Cao, and Xiyuan Song

Cite This: *ACS Omega* 2024, 9, 39259−39276

Read Online

ACCESS | Metrics & More | Article Recommendations

ABSTRACT: The high viscosity of heavy crude oil has been an obstacle to its safe production and economic transportation. In this work, a screened emulsified viscosity reducer system is conducted. Experimental results demonstrate that the most effective viscosity reducing agent comprises sodium oleate (NaOl) and cocamidopropyl betaine (CAB-35) in a ratio of 1:2, achieving a viscosity reduction rate of 94.65%. Additionally, the interfacial tension between oil and water decreases from 27 to 4 mN/m with 0.1 mass % TEOA and NaOH in a 1:1 ratio. The oil droplet size is uniformly distributed with D_{mean} is 14 μm and D_{50} is 11 μm. Droplets flocculate as the salinity increases to 0.2 mol/L, which corresponds to the apparent increase of viscosity. The adsorption of long alkyl chain lipophilic groups on surfactant molecules at the oil−water interface and the water film alters the wettability of pipe steel to water-wet, further enhancing the application of emulsification and viscosity reduction effects. The primary mechanism behind the viscosity reduction in emulsification is attributed to strong electrostatic interactions stemming from molecular electrostatic potential distributions.

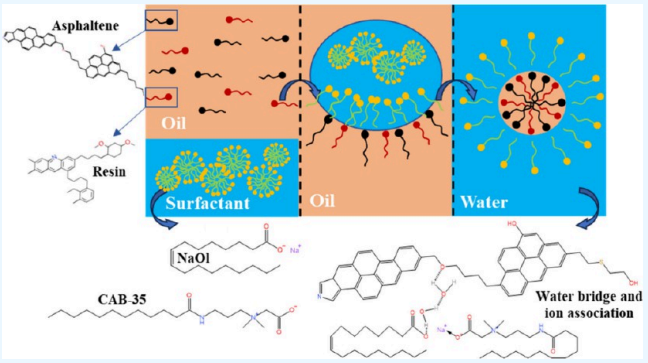

1. INTRODUCTION

Currently, the majority of recoverable oil resources in many countries are heavy crude with API degrees between 10.1 and 22.3.[1] Large-scale heavy crude oil reservoirs have been discovered in multiple blocks and layers in the South China Sea with continuous exploration (Figure 1). However, the poor fluidity of heavy crude oil in pipelines makes it difficult to deliver economically and efficiently. Various viscosity reduction technologies have been investigated to tackle these challenges, such as diluting light oil, pipe heating, microwave heating, modification, using viscosity reducers, and microbial viscosity reduction. Offshore platforms encounter space constraints and demand efficient transportation and construction of raw materials. Consequently, surfactant emulsification viscosity reduction has emerged as a viable option due to the availability of materials and the simplicity of the process.

The mechanical stirring disperses the heavy crude oil into small droplets, with the surfactant aqueous solution acting as the continuous phase. This emulsification process effectively reduces the apparent viscosity by converting friction between oil droplets into water films. Emulsifying viscosity reducers can be classified into various types based on their groups and compositions, including anionic, cationic, zwitterionic, and nonionic. Each type has its own set of advantages and disadvantages.[2] Screening and application of emulsion viscosity reducers have been conducted in recent decades. The applications and mechanisms of surfactants in different oil fields are summarized in Table.1.

Traditional surfactants have undergone extensive research and have shown a beneficial impact on reducing viscosity. However, certain limitations have been observed such as poor salt tolerance for anionic surfactants, high prices for cationic surfactants, and cloud points for nonionic surfactants. Therefore, it becomes crucial to employ a compounding method to overcome the drawbacks associated with individual agents.[17] Ma[18] evaluated the viscosity reduction effect of zwitterionic cocamidopropyl sulfobetaine (CSB) and anionic sodium dodecylbenzenesulfonate (SDBS) on Shengli heavy crude oil. The combination of CSB and SDBS can be closely arranged at the heavy crude oil−water interface, which enhances the strength of the interface film. Si[19] synthesized the anionic-nonionic surfactant SYW using 1,3 propylene glycol polyether (PPG), boric acid, maleic anhydride (MA), and sodium metabisulfite. SYW demonstrated a significant viscosity reduction of 98.6% in Xinjiang crude oil. Some references

Received: July 31, 2024
Revised: August 22, 2024
Accepted: August 30, 2024
Published: September 6, 2024

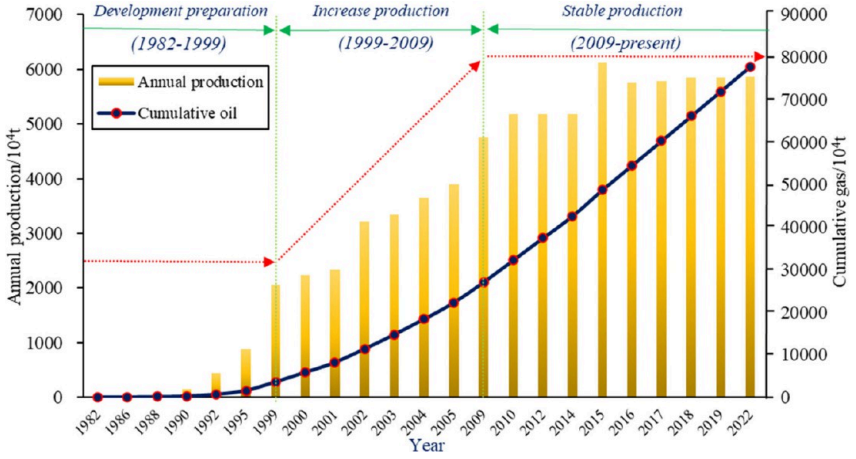

Figure 1. History of offshore oil and gas production in China.

Table 1. Application and Characteristics of Oilfields with Different Viscosity Reduction Methods

Type	Characteristics	Applications	Surfactant	Viscosity reduction effect	Viscosity reduction mechanism
Anionic	High output Low prices	PT. Pertamina EP Asset[3]	SLS	53.9%(DR)	Molecules attached to the interface film and form the electric double layer to enhance the droplet electrostatic repulsion[4]
	Material availability	Western Indian oilfield[5]	SDS	>99%	
	Renewable and biodegradable	Xinjiang oilfield[6]	SDS	>90%	
		Bohai oilfield[7]	AAGASs	96.8%	
Cationic	Little effect on heavy oil	Egyptian waxy crude oil[8]	Bola form	81.84%	Salting-out effect to change the driving force and mostly used in recovery enhancing[9]
	Good compatibility	Iranian oilfield[10]	CTAB	/	
	Easily react with alkali				
	Limited adaptability				
Zwitterionic	High surface activity	Indonesia T-KS[11]	SAE	/	The ionic groups regulate electrostatic interaction o realize $\pi-\pi$ stacking[12]
	Low toxicity	Tahe oilfield[13]	$RCOO^{-}DMEAH^{+}$	98.4%	
	Low irritation				
	Good salt tolerance				
Nonionic	High output	Liaohe oilfield[14]	AOS	98.89%	Molecules attached to the interface film and form micelles[15]
	High stability Good compatibility	Indian Mehsana oilfield[16]	Madhuca longifolia	70.84% (DR)	
	Has "cloud point"				

report different structural surfactants for viscosity reduction and emulsification of heavy oil such as different chain lengths[20] and electrical properties.[21]

Alkali is also used as a synergistic agent to reduce heavy crude oil viscosity by reacting with the acidic components[22] and reducing the interfacial tension.[23] Additionally, surfactant and alkali can also improve the wettability of rock and pipeline surface,[24] leading to enhanced transportation efficiency and cost reduction.[25] Gao[26] compounded CAO-15, sodium oleate and NaOH. It resulted in a significant reduction in viscosity rate by 97.46% and a decrease in pour point by 25 °C. Liu[27] optimized a compound system of fatty alcohol polyoxyethylene (AEO-12), sodium dodecyl sulfate (SDS) and NaOH for Liaohe heavy crude oil. This system significantly reduced the size of oil droplets to 0.2 μm and the interfacial tension to 0.008 mN/m. The addition of alkali enhanced the stability of the emulsion by tightly arranging the surfactant ion diffusion layer. Further research is still needed to investigate the varying effects on viscosity as there is currently no consensus.[28] For instance, Abdurahman[29] observed a slight increase in viscosity as the pH went from 5 to 8. While, Kumar[30] found a reduction in viscosity as the pH increased from 7 to 11. Pu[31] suggested that the viscosity of the emulsion would decrease under acidic and alkaline conditions.

Current research predominantly focuses on the mechanism of viscosity reduction through the single surfactant agent or binary surfactants interaction. Zhang[32] conducted molecular dynamics simulations to reveal that anionic surfactants interact

https://doi.org/10.1021/acsomega.4c07009
ACS Omega 2024, 9, 39259−39276

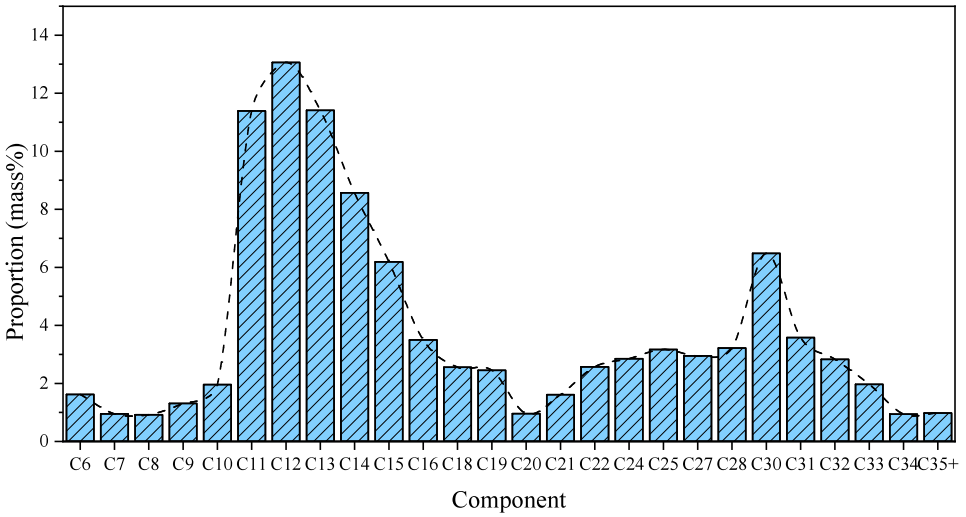

Figure 2. Oil hydrocarbon components distribution.

with polar macromolecules through weak dipole−dipole force, CH−π interaction and N−O interaction. Cai[33] observed challenges in achieving lower interfacial tension on the decane-water surface with a single amphoteric betaine. The competitive adsorption occurs between betaine and anionic surfactant, leading to an increased density of interface surfactant molecules. Zhang[34] synthesized an amphiphilic copolymer that weakly interacts with asphaltene disrupting asphaltene association structures and extending distances between asphaltene groups to achieve viscosity reduction in O/W emulsions. Wang[35] demonstrated that the nonionic viscosity reducer TPVR7 and anionic disuccinimide suberate (DSS) can enhance the anticoalescence performance of oil droplets in emulsions and strengthen interfacial films. The hydrophilicity of the viscosity-reducing agent group promotes its adsorption on the interface film. However, interactions between the two agents are not considered.

Current research on O/W emulsions primarily focuses on Newtonian fluids with a water content exceeding the inversion point. However, in practical applications, the water content for reducing the viscosity in heavy crude oil emulsions is typically around 30%. Additionally, the diverse components of oil pose challenges in using existing surfactant systems as a reference. While there is extensive research exploring the detailed mechanisms of viscosity reduction, there is a lack of substantial evidence at the molecular scale and standardized evaluation criteria. Therefore, it is essential to explore different surfactants and viscosity reduction mechanisms to streamline the screening process of viscosity reducers and reduce the costs associated with industrial applications.

This study focuses on the alkali-sensitive characteristics of anionic and zwitterionic surfactants to achieve stable emulsification and viscosity reduction of heavy crude oil. It is determined that the optimal anionic-zwitterionic-alkali surfactant agent is composed of NaOl, CAB-35, TEOA, and NaOH by evaluating the viscosity reduction rate. Microscopic/scan electron microscope observation (SEM), interfacial tension test, and molecular simulation are conducted to identify the morphological transformation of emulsion droplets and the mechanism of surfactant synergism. The insights obtained from this investigation provide valuable knowledge for engineers in comprehending the impact of emulsification factors and mechanisms on alleviating crude oil pipeline transportation consumption.

2. EXPERIMENTAL SECTION

2.1. Materials and Test Instruments. Degassed and dehydrated heavy crude oil is from the South China Sea. The surfactant reagents obtained as follows, anionic surfactants sodium dodecyl sulfate (SDS), sodium dodecyl benzenesulfonate (SDBS), sodium alpha-olefin sulfonate (AOS), sodium oleate (NaOl), fatty alcohol polyoxyethylene ether sulfate Sodium (AES), sodium fatty alcohol polyoxyethylene ether carboxylate (AEC), zwitterionic surfactant cocamidopropyl betaine (CAB-35), dodecyldimethyl betaine (BS-12), nonionic surfactants sorbitan monolaurate (Span-20), octylphenol polyethylene ether (Triton X-100), polysorbate (Tween-80) and octylphenol polyoxyethylene ether 10 (Op-10). The surfactant reagents are purchased from Shandong Yousuo Chemical Co., ltd.

2.1.1. Density. The heavy crude oil density is measured using a 10 mL pycnometer, an electronic balance, and a thermostatic water bath. Sample density at different temperatures is operated steps are as eq 1. The heavy oil density at 20 °C is 939.75 kg/m^3.

$$\rho_o = \frac{m_o - m_p}{V_p} \tag{1}$$

where ρ_o is the oil sample density, kg/m^3; m_0 is the quality of pycnometer and oil sample, kg; m_p is the quality of pycnometer, kg; and V_p is the volume of pycnometer, 10 mL.

2.1.2. Viscosity. The coaxial cylinder rotor, coaxial cylinder, and HAAKE intelligent rheometer are used to assess the viscosity of heavy crude oil. The shear rate is set as 0−1000 s^{-1} and the temperature is set as 20−90 °C driven by the heating module and the rotating module of the rheometer. The heavy oil viscosity is 5047.52 mPa s at 20 °C.

2.1.3. Saturates, Aromatics, Resins, and Asphaltene (SARA). The heavy crude oil is divided into four components according to the "NB/SH/T0509−2010 Test method for separation of asphalt into four fractions". The N-heptane, toluene, and ethanol are used to flush through the adsorption column which is filled by activated alumina. The mass fraction of asphaltene, saturates, aromatics, and resins are 22.07%,

https://doi.org/10.1021/acsomega.4c07009
ACS Omega 2024, 9, 39259−39276

48.07%, 18.17%, and 11.69%, respectively. High levels of colloidal asphaltenes can affect the crude oil viscosity.

2.1.4. Hydrocarbon Component. Oil hydrocarbon components are tested by Agilent 7890A chromatograph. The heavy crude oil is poured into the beaker, sampled with a 10 μL microinjector, and injected into the chromatograph. As shown in Figure 2, the carbon number distribution of heavy oil exhibits a broad range with the peak content observed at C12, accounting for 13.06 wt %. Oil density, viscosity, SARA and component properties are summarized in Table 2.

Table 2. Properties of Heavy Crude Oil

Test	Value	Compound	Fraction (wt %)
Density (kg/m^3)	939.75 (20 °C)	C_6–C_{10}	6.76
Viscosity (mPa s)	5047.52 (20 °C)	C_{11}–C_{15}	50.62
Saturates (wt %)	48.07	C_{16}–C_{20}	9.47
Aromatics (wt %)	18.17	C_{21}–C_{25}	10.20
Resins (wt %)	11.69	C_{26}–C_{35+}	22.95
Asphaltene (wt %)	22.07	$\sum C_n$	100.00

2.2. Preparation of Samples. O/W emulsions are prepared by the HH-4 digital display constant temperature water bath (Changzhou Guohua Electrical Appliance Co., Ltd.) and GJ-3S digital display electronic stirrer (Qingdao Xinruide Petroleum Instrument Co., Ltd.). Initially, the crude oil and surfactant solution are preheated in the water bath to 30 °C for one hour. Subsequently, 70 mL of oil is uniformly injected into 30 mL of surfactant solution at a stirring rate of 1000 r/min and a stirring time of 90s. After addition of all the crude oil, the mixture is stirred for an additional 90s. The oil samples, solution samples, and prepared emulsions are tested for rheology, surface tension, and microscopic properties. The experimental process is summarized in Figure 3.

2.3. Experimental Device and Processes. *2.3.1. Rheological and Water Separation Evaluation.* Different types of rotors and cylinders are used for emulsions with varying viscosities, as shown in Figure 4. The coaxial cylinder rotor and coaxial cylinder are employed for heavier emulsions (Figure 4a and Figure 4c). The double slit rotor and double slit cylinder are used for low viscosity O/W emulsions (Figure 4b, Figure 4d). The emulsion samples prepared in section 2.2 are immediately transferred to the rheometer. The shear rate is set as 0−1000 s^{-1} and the temperature is set as 20−90 °C. The viscosity reduction rate is calculated according to the following eq 2.

$$\delta = \frac{\eta_o - \eta_e}{\eta_o} 100\% \tag{2}$$

where δ is viscosity reduction rate, %; η_o is the viscosity of crude oil, mPa s; η_e is the viscosity of emulsion, mPa s.

The emulsion prepared in Section 2.2 is transferred to a 100 mL test tube (Figure 4f). Initially, the total height of the emulsion is measured, followed by hourly measurements of the height of separated water. The water separation rate of the emulsion is determined using eq 3.

$$f = (v_1/v_2)100\% = (h_1/h_2)100\% \tag{3}$$

where f is the water separation rate, %; v_1 is the volume of precipitated water, mL; v_2 is the total volume of emulsion, mL; h_1 is the height of precipitated water, cm; and h_2 is the total water height, cm.

2.3.2. Interfacial Tension Test. As shown in Figure 5, the JC2000D2 contact angle measuring instrument (Shanghai Zhongchen Digital Equipment Co., Ltd.) is utilized to measure the surface tension and interfacial tension at the temperature of 30 °C. The microsyringe is installed on the fixed frame to control the oil output being 3 μL each time (Figure 5a). The data are recorded once the shape of oil droplet stabilized and measured by the pendant-drop method (Figure 5b).

2.3.3. Droplet Size and Distribution Analysis. As depicted in Figure 6a, the transmission and reflection polarizing microscope (Shanghai Cai Kang Optical Instrument Co., Ltd.) is used to observe the O/W emulsion. The objective lens

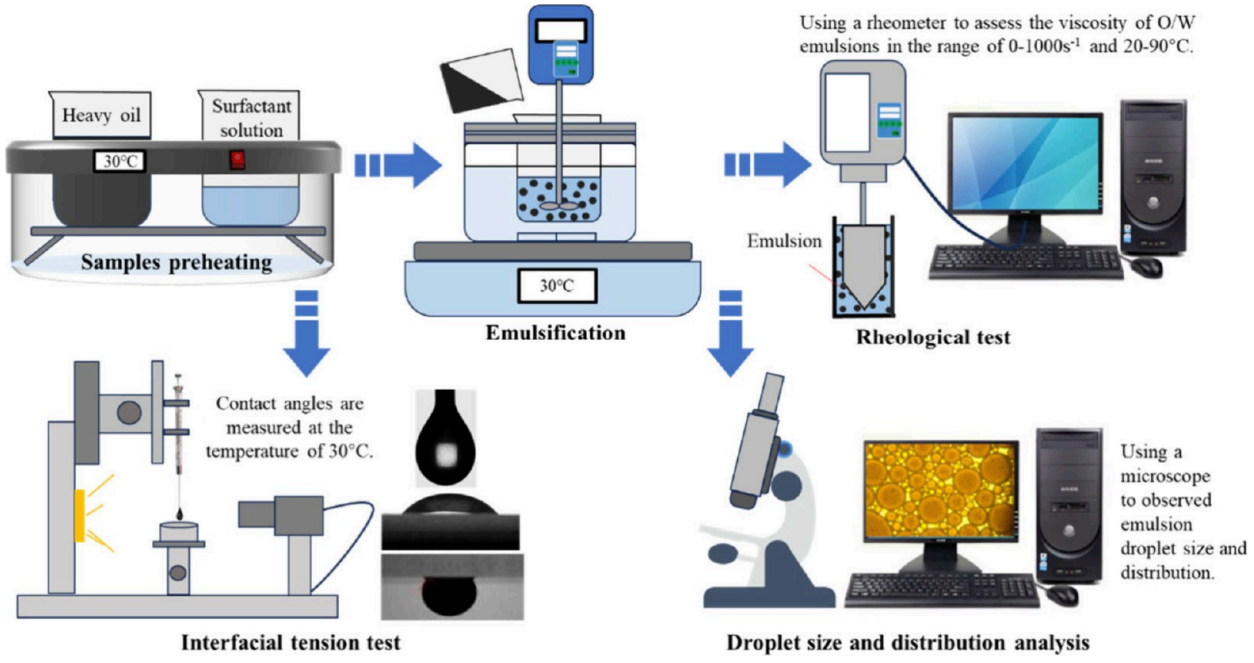

Figure 3. Experimental process for sample preparation and characterization test.

https://doi.org/10.1021/acsomega.4c07009
ACS Omega 2024, 9, 39259−39276

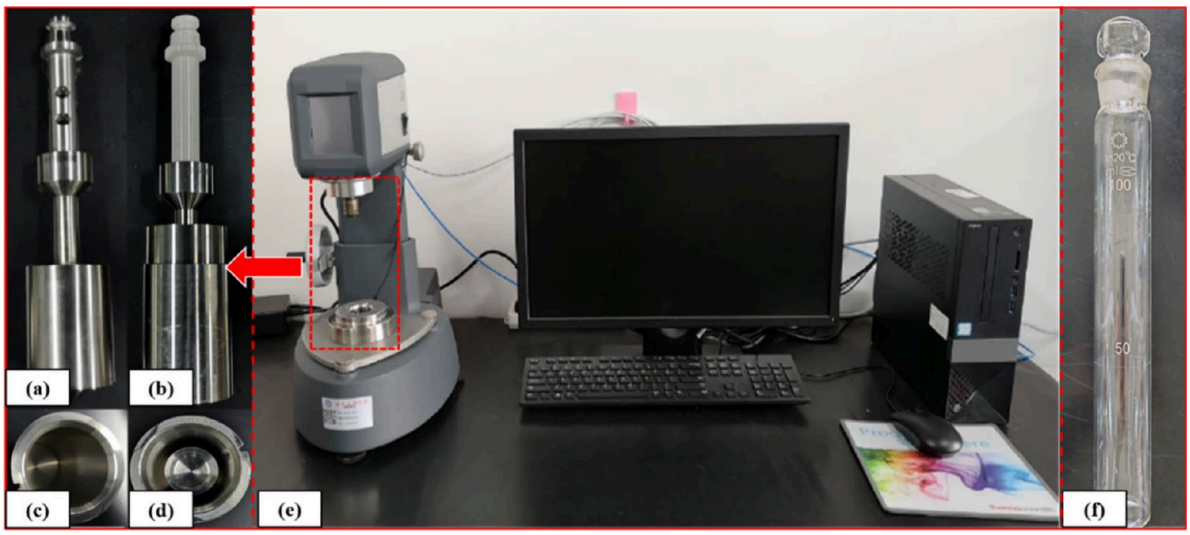

Figure 4. rheometer components and test tubes: (a) coaxial cylinder rotor; (b) double slit rotor; (c) coaxial cylinder; (d) double slit cylinder; (e) rheometer; (f) test tube.

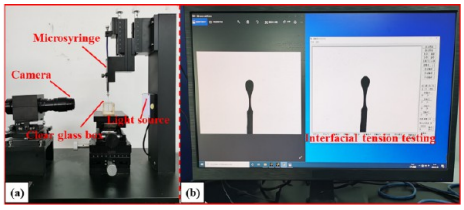

Figure 5. Interfacial tension test components: (a) testing device; (b) captured image.

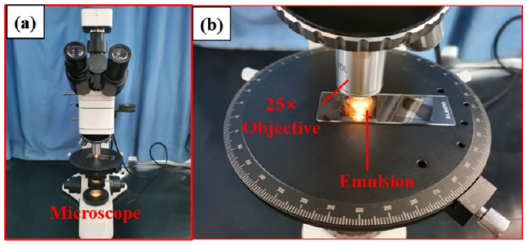

Figure 6. Microscopic observation. (a) Microscope; (b) eyepiece and emulsion slide.

had magnifications of 10, 25, and 60 times, corresponding to the droplet size (Figure 6b). The mean droplet diameter (D_{mean}) and median droplet diameter (D_{50}) are evaluated by ImageJ software.

2.3.4. Morphology Analysis at Micrometer-Scale. Scanning electron microscopy (SEM) is utilized to examine the microscopic morphology of crude oil and emulsion on the pipe surface (Figure 7). The materials undergo pretreatment with drying and gold spraying. Subsequently, the sample is chemically characterized and elementally analyzed using Energy Dispersive Spectroscopy (EDS). Elements are identified based on the peak positions in the spectrum, with signal intensity reflecting element concentration.

2.3.5. MD Simulation Methodology. Asphaltene molecules are distinguished by the presence of hydroxyl groups, ketone groups, and heteroatoms, all of which significantly have a notable influence on the physical characteristics of crude oil. Researchers commonly rely on the average molecular structure to study asphaltene mixtures. The classic molecular structure model of asphaltene is presented by Jia.[36] The molecular structures of surfactants and asphaltene are shown in Figure 8. The density functional theory (DFT) DMol^3 program in Materials Studio is utilized to investigate the electrostatic potential of surfactants and asphaltene molecules. The interactions between molecules are obtained by using the Forcite module. For DMol^3 settings, surfactant and asphaltene molecules are optimized using the Generalized Gradient Approximation (GGA) with a fine quality energy of 10^{-5} Ha, maximum of 500 iterations, and a maximum step size of 0.3 Å. For Forcite settings, the smart algorithm is employed, utilizing the COMPASS III force field with an energy of 0.001 kcal/mol and a force of 0.5 kcal/mol/Å. The geometry-optimized asphaltene molecules are annealed using the Anneal module through 10 cycles in the COMPASS III force field of the NVT ensemble at temperatures ranging from 300 to 500 K. The electrostatic and van der Waals force are calculated using the Atom-based algorithm, with a time step of 1 fs, Nose thermostat at 298 K, and initial random speed.

3. RESULTS AND DISCUSSION

3.1. Effects of Surfactant Type and Compounding on Viscosity. The O/W emulsion preparation is carried out under the following conditions: deionized water with a mass fraction of 1% surfactants, emulsification temperature of 30 °C, and stirring rate of 1000r/min. Different surfactants exhibit varying effects as shown in Figure 9a. These emulsions are considered to be shear dilution fluids. Notably, the anionic surfactant NaOl, the zwitterionic surfactant CAB-35, and the nonionic surfactants Span-20, demonstrate significant viscosity reduction effects of over 90%. Figure 9b illustrates the water separation rates of emulsions over a 6 h period. The water separation rates for individual agent emulsions of NaOl and CAB-35 are 47.01% and 49.56% respectively, while Span-20 and OP-10 exhibit rates of 59.21% and 60.32%. To further investigate viscosity changes in the emulsion, NaOl and CAB-35 are used as primary agents, supplemented by Span-20 and OP-10.

The effect of compounding two surfactants is shown in Figure 10. The combination of NaOl and CAB-35 at a mass ratio of 1:2 has the best viscosity reduction effect, with the

https://doi.org/10.1021/acsomega.4c07009
ACS Omega 2024, 9, 39259−39276

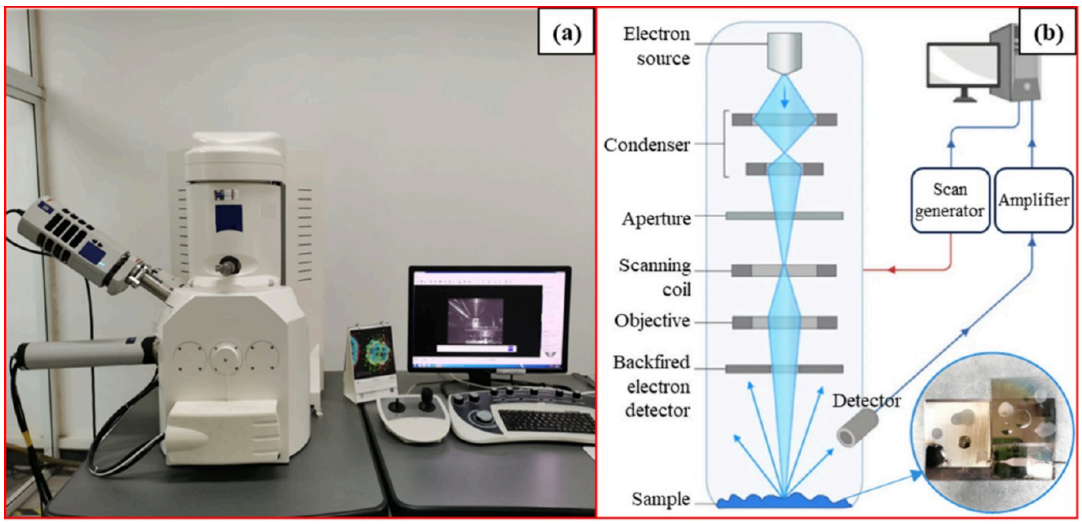

Figure 7. SEM analysis. (a) EVO MA 15 SEM; (b) SEM structure and samples.

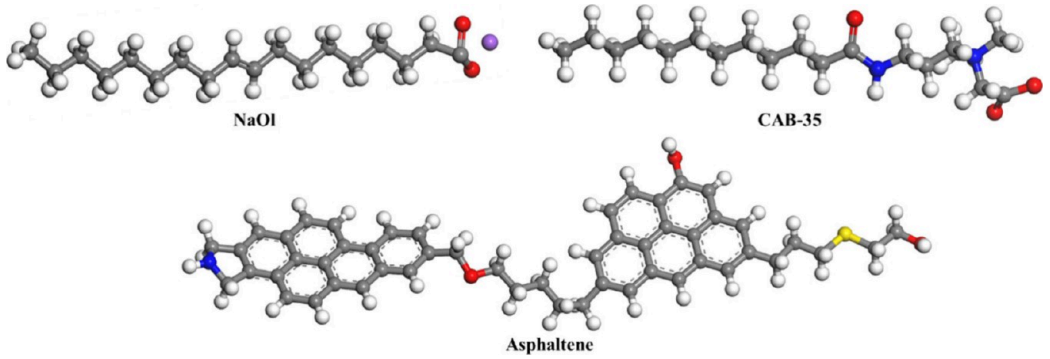

Figure 8. Molecular structures of asphaltene and surfactants. (atom color: gray, C; white, H; red, O; yellow, S; blue, N; purple, Na).

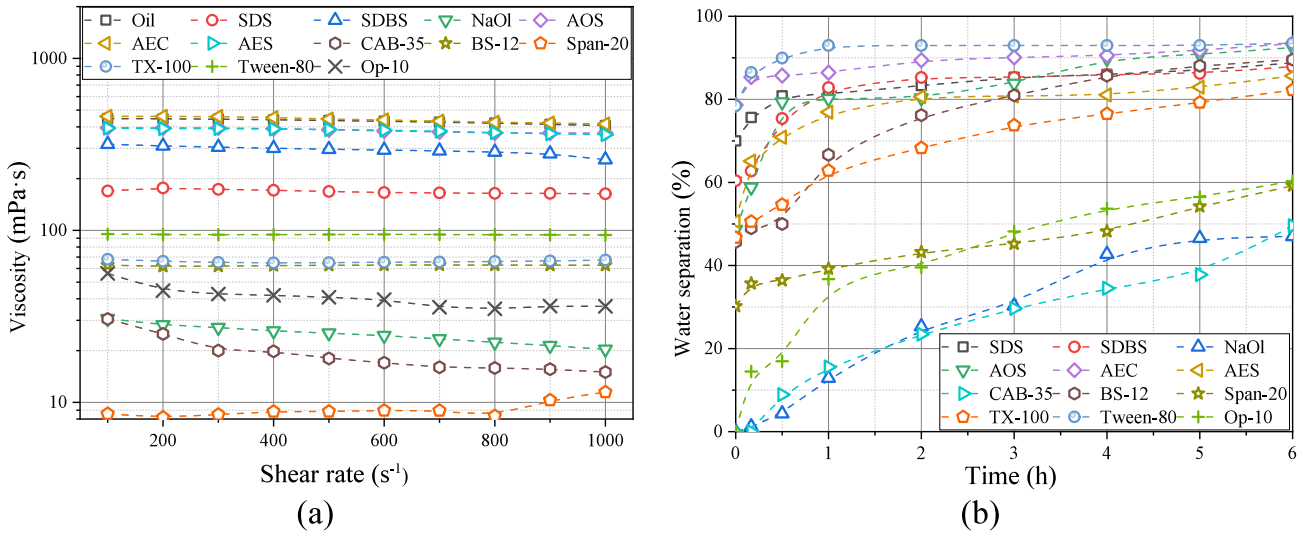

Figure 9. Impact of surfactant single agent type on viscosity and water separation. (a) Emulsion viscosity; (b) water separation rate.

viscosity reduction rate is 94.65%. NaOl aqueous solution is alkaline and can be partially hydrolyzed into NaOH to react with the petroleum acid in heavy oil. The carboxylate and the double bond can increase the curvature of the oil−water interface film.[37] It is more conducive to emulsification and viscosity reduction. Additionally, the molecular structure of CAB-35 contains both anionic and cationic polar functional groups, which enhances its water hardening ability.[38] CAB-35 also exhibits a significant viscosity reduction effect both as a standalone agent and in combination with anionic NaOl. The compounds of NaOl and CAB-35 are selected for subsequent experiments due to the compatibility.

3.2. Effects of Emulsification Conditions on Viscosity.

3.2.1. Surfactant Content. According to the results presented

https://doi.org/10.1021/acsomega.4c07009
ACS Omega 2024, 9, 39259−39276

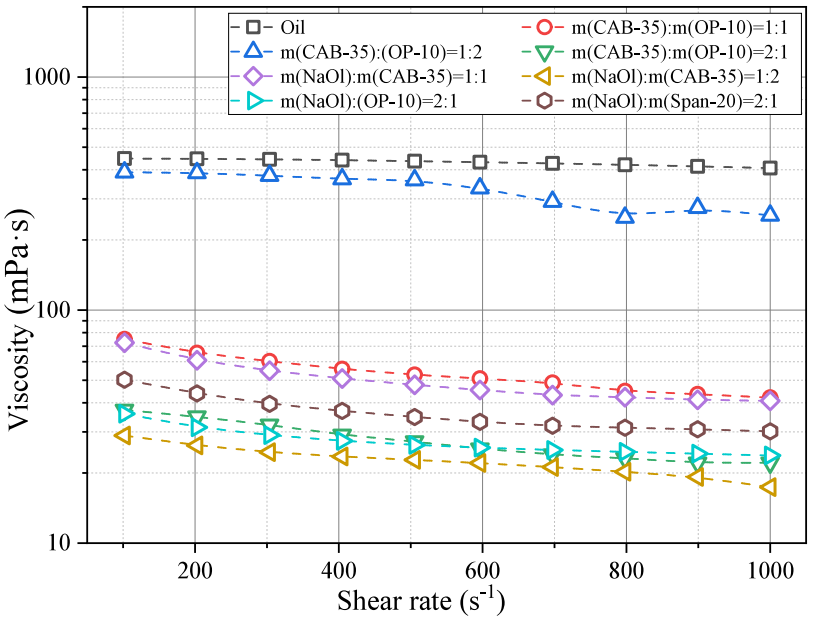

Figure 10. Impact of the compound surfactant agent type on viscosity.

in Figure 11, the emulsion viscosity initially decreases and then increases as the surfactant concentration increases. The most

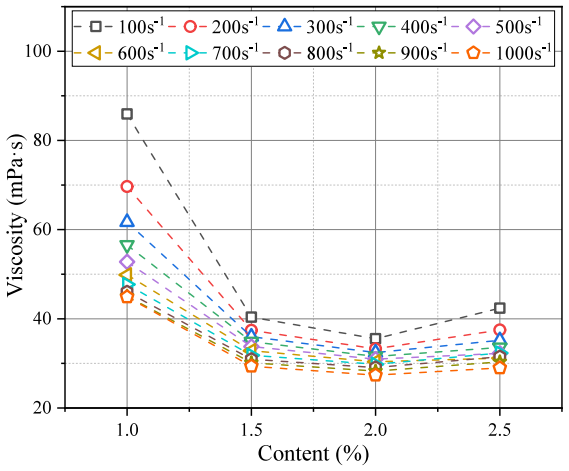

Figure 11. Impact of compound mass fraction of the surfactant agent on viscosity.

significant reduction in viscosity occurs at a surfactant concentration of 2%. This can be attributed to the gradual increase in the number of surfactant molecules adsorbed on the oil−water interface prior to the concentration of 2%. The interface film strength gradually improves, leading to a reduction in viscosity.[39] However, at higher surfactant concentrations, the effect of adsorption on the heavy components in the crude oil becomes saturated. Consequently, additional surfactant molecules will contribute to an increase in the viscosity of the external phase, leading to an overall increase in the emulsion viscosity.[40] Given that a surfactant content of 1% effectively reduces viscosity, we subsequently use 1% as the baseline concentration to minimize costs in a follow-up experiment.

3.2.2. Alkali Type and Content. The inorganic bases NaOH, Na_2CO_3 and organic base TEOA are selected to carry out viscosity reduction experiments with the mass fraction of 0.1−0.5%. Figure 12 illustrates the effect of these substances on viscosity reduction. The optimal viscosity reduction rates are observed at 94.95% (0.1% NaOH), 93.53% (0.3% Na_2CO_3), and 94.13% (0.2% TEOA), respectively. Polar functional groups present in heavy oil, such as colloids, asphaltenes, naphthenic acids and fatty acids have the ability to ionize easily with alkali.[41] As a result, active substances are formed that can work in synergy with the existing surfactant compounding system. It stabilizes a greater number of oil−water interfaces, leading to a more even dispersion of oil droplets with smaller particle sizes. The hydrolysis ionization equilibrium equations of the three bases are shown as eqs 4 to 7.

$$NaOH \rightleftharpoons Na^+ + OH^- \quad (4)$$

$$Na_2CO_3 \rightleftharpoons 2Na^+ + CO_3^{2-} \quad (5)$$

$$CO_3^{2-} + H_2O \rightleftharpoons HCO_3^- + OH^- \quad (6)$$

$$R\text{-}NH_2 + H_2O \rightleftharpoons OH^- + R\text{-}NH_3^+ \quad (7)$$

In the case of strong alkali (NaOH), the viscosity of the emulsion increases with rising alkali content. Conversely, for weak alkalis (TEOA and Na_2CO_3), the emulsion viscosity initially decreases, before subsequently increasing. Among the three alkalis, NaOH is a fully ionized strong base that generates the highest number of surface-active substances and exhibits the strongest stabilizing effect. Weak bases have a limited ability to react with macromolecular acidic substances. And low concentrations of alkali cannot fully ionize the petroleum acid in heavy oil. Consequently, as the alkali concentration increases, the dissociation effect gradually strengthens. It leads to the decrease in emulsion viscosity once the concentration reaches the optimal viscosity reduction rate.[42] However, as the alkali concentration continues to increase, the balance between dissociated and undissociated acids is disrupted, resulting in the decrease in the effectiveness of viscosity reduction.

Surfactant solutions are prepared consisting of 1% NaOl and CAB-35 at a mass ratio of 1:2, combined with various alkalis.

https://doi.org/10.1021/acsomega.4c07009
ACS Omega 2024, 9, 39259−39276

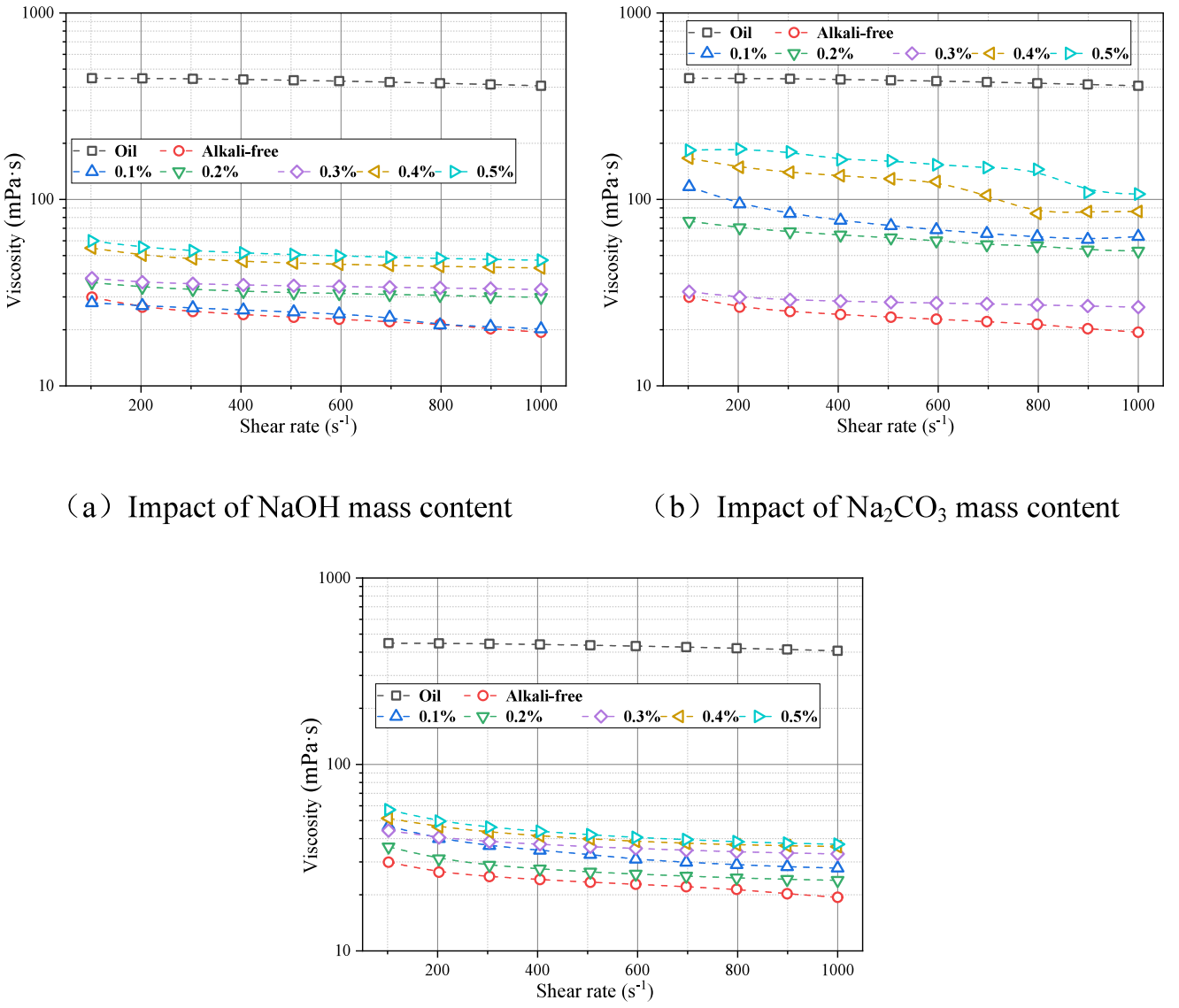

（a）Impact of NaOH mass content

（b）Impact of Na_2CO_3 mass content

（c）Impact of TEOA mass content

Figure 12. Impact of the alkali mass fraction on viscosity.

The crude oil is emulsified with the solution at a ratio of 7:3 at 30 °C and 1000 rpm. The emulsion is then transferred into a 50 mL colorimetric tube. Subsequently, the heights of the oil and solution phases are measured to calculate the water separating effect using the formula eq 8 provided below. The experimental results are presented in Table 3.

$$f = (v_1/v_2)100\% = (h_1/h_2)100\% \quad (8)$$

where f is the water separating rate,%; v_1 is the volume of precipitated solution, mL; v_2 is the volume of emulsion, mL; h_1 is the height of precipitated solution, cm; and h_2 is the height of emulsion, cm.

Table 3. Effect of Alkali Compound on the Water Separation Rate of Emulsions

System	TEOA:NaOH			TEOA:Na_2CO_3		
Ratio of alkali agents	2:1	1:1	1:2	2:1	1:1	1:2
24 h water separation rate (%)	7.24	2.50	5.02	16.32	17.15	21.60

As shown in Table 3, a low-corrosive organic base is combined with inorganic bases at a concentration of 0.1%. The emulsion containing TEOA and NaOH, mixed in a 1:1 ratio, exhibited the lowest water separation rate after 24 h, measuring only 2.50%. Consequently, this formulation has been selected as the alkaline agent for this study to ensure the long-term stability and safe transportation of the emulsion on the offshore platform.

3.2.3. Oil–Water Ratio. Emulsions at oil–water ratios of 9:1, 8:2, 7:3, 6:4, and 5:5 are selected for viscosity reduction experiments. As shown in Figure 13, the emulsion quickly inverts into the water-in-oil (W/O) type when the oil–water ratio is 9:1. At this point, the surfactant has no viscosity-reducing effect. As the oil/water ratio decreases, the influence of water on the viscosity gradually increases. The emulsion viscosity also decreases with the shear weakened dilution effect.

https://doi.org/10.1021/acsomega.4c07009
ACS Omega 2024, 9, 39259−39276

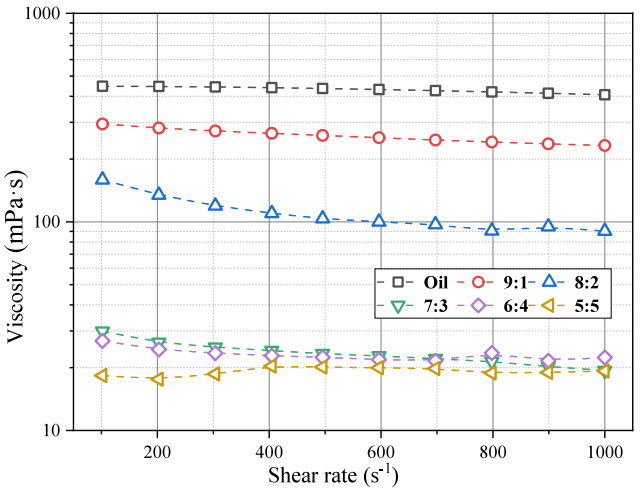

Figure 13. Impact of the oil−water ratio on viscosity.

Sufficient surfactant molecules can generate and stabilize a larger oil−water interface area, resulting in smaller oil droplets and increased droplet separation distance.[43] It leads to a reduction in collision frequency and frictional resistance, ultimately reducing the apparent viscosity of the emulsion. From safety and economic standpoint, it is preferable to maintain an oil/water ratio of 7:3. Increasing the content beyond this ratio will not significantly reduce the emulsion viscosity.

3.2.4. Emulsifying Temperature. The viscosity reduction effects at emulsification temperatures of 30 °C, 50 and 70 °C are shown in Figure 14. As the temperature increases, the

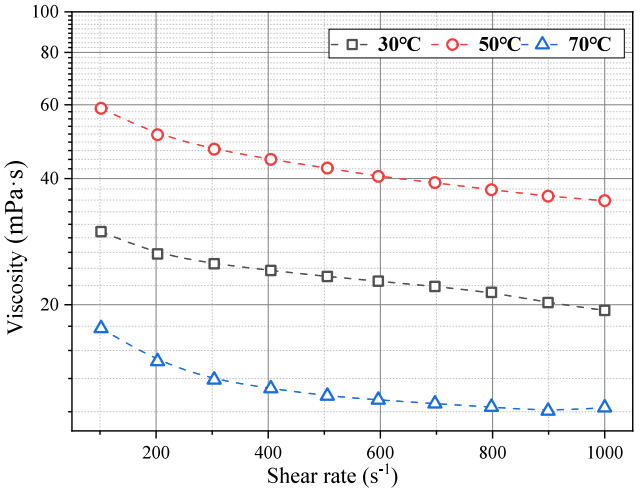

Figure 14. Impact of emulsifying temperature on viscosity.

emulsion viscosity initially increases and then decreases. The temperature-dependent effect on viscosity reduction can be attributed to the impact on the internal phase viscosity, the dissolution and adsorption effect of surfactant molecules at the interface, and the Brownian motion. Specifically, the increase in temperature enhances the solubility of surfactant molecules at the interface within the range of 30 to 50 °C. It strengthens the oil−water interface film and increases the shear resistance during rheological analysis. The macroscopic performance is characterized by an increase in the viscosity. The continuous increase in temperature causes polar substances to become more soluble and weakens the associations adsorbed on the oil−water interface. As a result, the surface charge density of the oil droplets decreases, and the repulsion weakens. The distribution of surfactant molecules on the oil−water interface film is looser. Besides, the enhanced Brownian motion of oil droplets leads to faster aggregation and sedimentation.[44] The water phase wrapped in the oil droplets also accelerates to precipitate. Therefore, 30 °C is identified as the most suitable emulsification temperature.

3.2.5. Stirring Rate. The effects of stirring rate at 500, 1000, and 1500 rpm on viscosity reduction are shown as Figure 15.

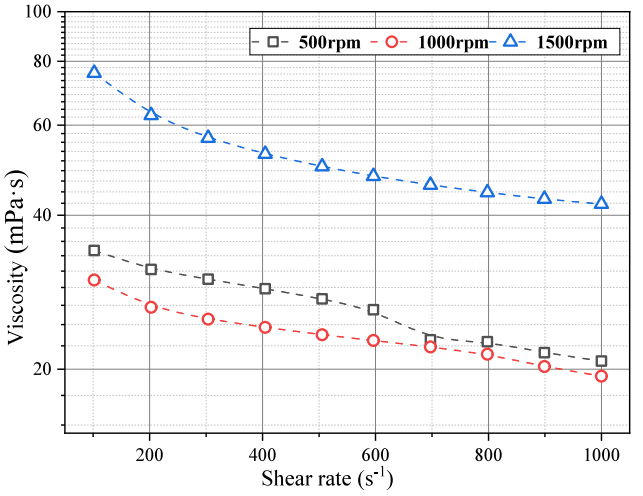

Figure 15. Impact of stirring rate on viscosity.

The results indicate that the emulsion viscosity initially decreases and then increases significantly as the stirring rate rises. This phenomenon can be attributed to the fact that an optimal stirring rate (1000 rpm) promotes the uniform distribution of oil droplets.[45] However, an excessive stirring rate leads to a smaller particle size and a larger number of dispersed droplets. This excessive dispersion overconsumes the limited surfactant molecules,[46] resulting in a loose arrangement of the interface film and a reduction in strength. Consequently, the O/W emulsion becomes unstable and undergoes phase reversal, leading to an increase in the viscosity.

3.2.6. Inorganic Salt Type and Content. Formation water contains a significant amount of inorganic salt ions. The type and content of these ions play a crucial role in the hydrophobic effect, alkali loss, and double electric layer. The inorganic salts (NaCl, KCl, $CaCl_2$, $MgCl_2$, Na_2SO_4, $NaHCO_3$, and Na_2CO_3) are selected as the research objects. The changes in the emulsion viscosity with different types and concentrations of ions are presented in Figure 16a. The viscosity of emulsions containing ions is higher compared to emulsions without ions. The data indicate an initial increase in emulsion viscosity, which is subsequently followed by a decrease as ion concentration rises. Turning points are observed at approximately 0.15 mol/L for bivalent cations and 0.2 mol/L for monovalent cations and anions. Ions increase the polarity of the continuous phase due to salting-out effect at low concentrations. It prompts the migration of surfactant molecules to the oil−water interface and strengthened the film. However, this effect hinders rheological shear, resulting in a slightly higher viscosity. The gradually increasing ion concentration also screens the electrostatic repulsions between

https://doi.org/10.1021/acsomega.4c07009
ACS Omega 2024, 9, 39259−39276

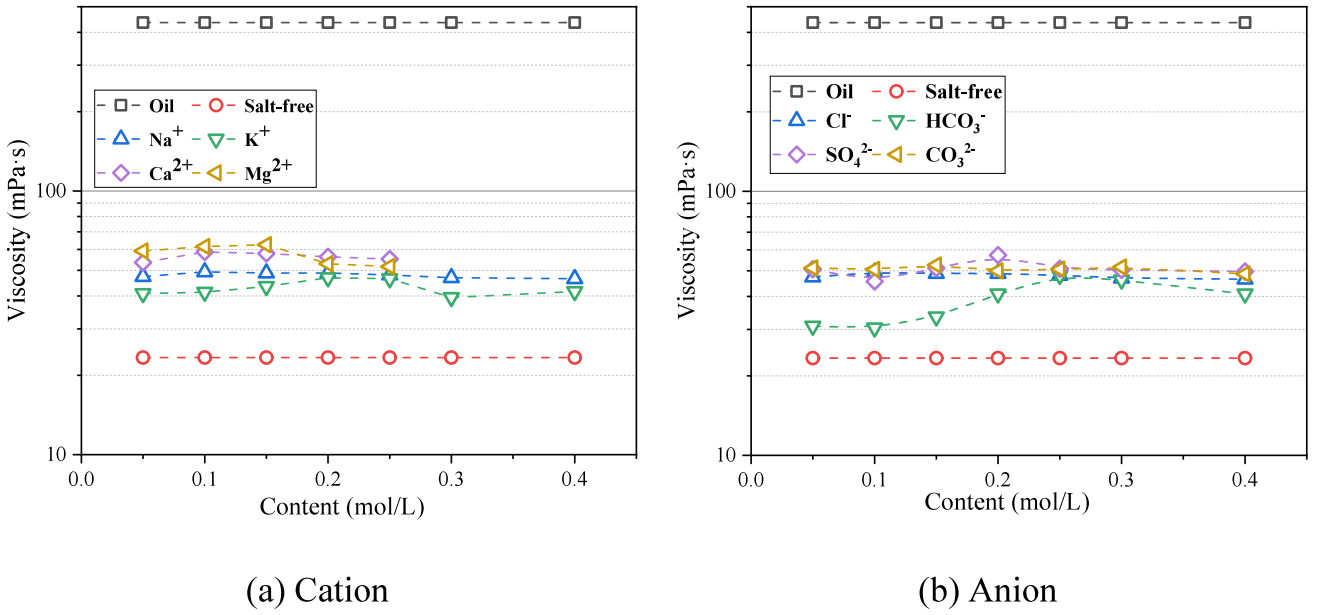

Figure 16. Impact of ion type and content on viscosity.

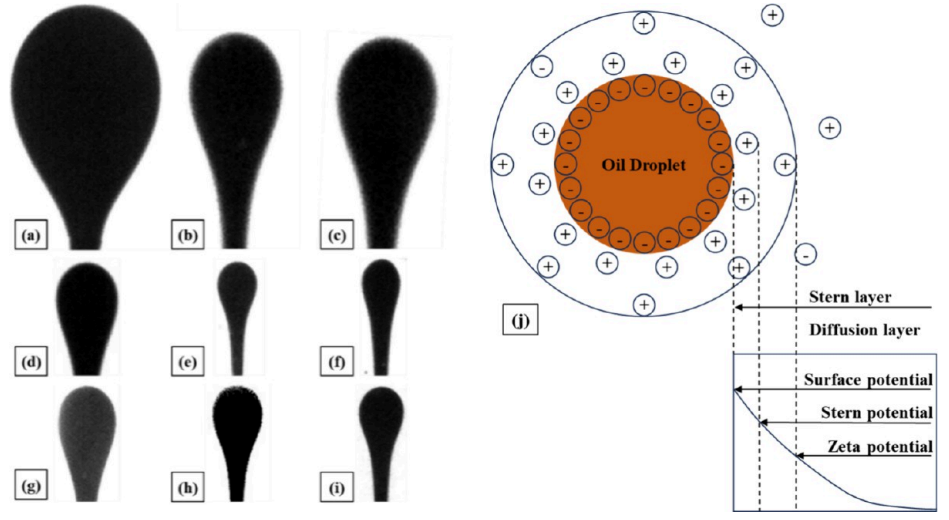

Figure 17. Interfacial tension between oil-solution and double electric layer. (a) oil-deionized water; (b) oil and 1% NaOl and CAB-35 (1:2); (c) oil-1% compounding system and 0.1% alkalis (TEOA:NaOH = 1:1); (d) alkali-free solution with 2000 mg/L salinity; (e) 10 000 mg/L salinity; (f) 20 000 mg/L salinity; (g) alkaliferous solution with 2000 mg/L salinity; (h) 10 000 mg/L salinity; (i) 20 000 mg/L salinity; (j) droplet double electric layer.

quaternary ammonium cations, enhances the lipophilicity of surfactant molecules.[47] Counter ions neutralize excessive surface charges, leading to a weakening of electrostatic repulsion between the droplets.

Ca^{2+} and Mg^{2+} ions can react with OH^- to form slightly soluble and insoluble substances, which reduces the effectiveness of active substances that stabilize the oil−water interface film.[48] Organic bases and high-valent cations can form complexes, reducing the consumption of OH^- in the surfactant solution. These combined effects result in a slightly higher emulsion viscosity with added Mg^{2+} and Ca^{2+} ions compared to the Na^+ and K^+ ions. As shown in Figure 16b, divalent anions have a more significant impact on the compression double electric layer and exhibit a stronger salting out effect compared to monovalent anions.[49,50] $NaHCO_3$ can undergo incomplete ionization and hydrolysis to generate OH^-. It promotes the reaction of acidic substances in heavy oil, leading to a lower apparent viscosity of the system.

3.3. Mechanism of Viscosity Reduction. *3.3.1. Interfacial Tension.* The interfacial tension between heavy oil and various solutions is presented in Figure 17 and Table 4. Initially, the interfacial tension between heavy oil and deionized water is measured to be 27 mN/m (Figure 17a), which significantly decreases to 4 mN/m after adding the surfactant solution (Figure 17b).

The introduction of 0.1% alkali substance results in a slight increase in interfacial tension due to changes in the molecular interaction between anionic and zwitterionic surfactants (Figure 17c). For alkaline conditions, the negative electrons of the carboxyl group of CAB-35 and the negative ions of the fatty acid group of NaOl associate through Na^+. Conversely, the quaternary ammonium salt cation of CAB-35 interacts with

https://doi.org/10.1021/acsomega.4c07009
ACS Omega 2024, 9, 39259−39276

Table 4. Interfacial Tension of Heavy Oil and Surfactant Solutions

Solution		Interfacial tension (mN/m)	Solution		Interfacial tension (mN/m)
Deionized water		27	0.1% Na_2CO_3		4.13
1% Compounding system (NaOl:CAB-35 = 1:2)		3.68	0.1% TEOA		5.07
0.1% Alkaliferous (TEOA:NaOH = 1:1)		3.74	0.1% NaOH		3.64
Alkali-free	2000 mg/L	3.38	Alkaliferous	2000 mg/L	3.30
	10000 mg/L	1.93		10 000 mg/L	3.19
	20000 mg/L	2.17		20 000 mg/L	2.58

the fatty acid anion of NaOl via ionic bonds. The interfacial tension between heavy oil and the TEOA solution is slightly larger due to the weaker ability to stabilize the interface.

The increase in mineralization contributes to a reduction in the interfacial tension (Figure 17d–i). Solutions containing 20 000 mg/L inorganic salts without alkali shows a decrease in IFT and increases to 2 mN/m. The viscoelasticity of surfactant solutions can be affected by the salinity, which in turn affects the mass transfer dynamics of surfactant and oil molecules at the oil–water interface.[51,52] This can be attributed to the formation of a double electric layer by surface active molecules adsorbed on the droplet surface and the salting-out effect (Figure 17j).[53] The thickness of the double electric layer is inversely proportional to the square root of the ion valence and concentration, as indicated in eq 9.

$$\kappa^2 = \frac{2e^2 \sum n_i Z_i^2}{\varepsilon KT} \tag{9}$$

where κ^{-1} is the equivalent thickness of electric double layer, m; e is the electronic charge, 1.6×10^{-19} C; n_i is the number of ions; Z_i is the ionic valence number; ε is the dielectric constant of the medium, F m^{-1}; K is Boltzmann constant; σ is the surface charge density, C m^{-2}.

The positively charged inorganic salt ions diffuse on the droplet surface, thereby compressing the thickness of the electric double layer. Consequently, the arrangement of surfactant molecules at the interface becomes more compact,[54] leading to alterations in the electrical repulsion between the oil droplets.[55,56]

3.3.2. Droplet Size Distribution. Microscopic images are taken of emulsion samples made with heavy oil and various solutions, as shown in Figure 18. The particle size distributions of oil droplets are illustrated in Figure 19, which can be summarized as reversion W/O emulsion, O/W emulsions, and flocculation. Taylor[57] described the deformation of the internal phase. The interface film of droplets is deformed by the external force, while the interfacial tension maintains the sphericity. The competition between these two factors determines the shape of the droplets. Two methods are employed to quantitatively study the influence of the oil droplet size and structures. The first method involves analyzing the mean droplet diameter (D_{mean}), while the second method focused on the droplet median diameter (D_{50}).

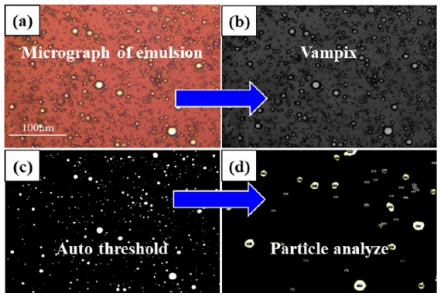

Figure 18. Measurement of particle size. (a) Micrograph; (b) Vampix; (c) auto threshold; (d) particle analyze.

Significant differences in droplet microstructure are detected in Figure 19. Figure 19a is prepared using an oil–water ratio of 9:1. In the W/O emulsions, the water droplet is small with the D_{mean} of 2.30 μm and the D_{50} of 1.88 μm (Figure 20a). The emulsion transformed into an oil-in-water type (Figure 19b) under the conditions of an oil–water ratio of 7:3, a mass fraction of 1% surfactant (NaOl: CAB-35 = 1:2). The oil droplets display an irregular spherical shape with a tail extending up to 300 μm. The D_{mean} is 57 μm, with the D_{50} value of 44 μm (Figure 20b). It can be observed that the size range of the oil droplets becomes narrower with the addition of alkalis in Figure 19c and Figure 20c. Additionally, there is less deformation on the outer surface, leading to an increase in roundness. A direct correlation among emulsion droplet size, emulsion stability and apparent viscosity has been revealed.[58] Smaller oil droplets are indicative of a more stable emulsion system. The experimental results presented in Section 3.2.2 confirm that the stability of alkali-added emulsions is enhanced. In Figure 19d and Figure 20d, it is observed that a large number of loose chain flocs appeared in emulsions with adding alkalis and inorganic salts. The small oil droplets are found to be distributed in a three-dimensionally manner around the larger droplets, and these oil droplets did not coalesce upon collision. Microscopic measurements revealed that the particle size distribution of the system became narrower after flocculation, where D_{mean} is 3 μm and D_{50} is 2 μm.

The degree of flocculation of oil droplets depends on the balance of attraction and repulsion, which mainly includes van de Waals, electrostatic, steric, depletion, and hydration.[59] The surfactants used in this study are anionic and zwitterionic, leading to a combination of van der Waals forces and electrostatic repulsion as the main repulsive effects. In the absence of the surfactants, the repulsive force is strong enough to counteract the van der Waals force, avoiding oil droplet flocculation. The attraction between droplets increases and the droplets start to flocculate as the salinity increases to 0.2 mol/L. This corresponds to the point where the viscosity transition occurs as observed in Figure 16.

Previous studies have suggested that the adsorption amount of active agents on the oil–water interface increases with the increase in ion concentration.[60] It results in a decrease in the effective radius of active substances. Therefore, at high ion concentrations (>0.2 mol/L) and low electrostatic repulsion, oil droplets tend to coalesce rather than flocculate,[42,61] leading to a decrease in emulsion viscosity.[62]

3.3.3. Micrometer-Scale Appearance. SEM and EDS are two commonly used advanced microscopic analysis techniques. In Figure 21, the micromorphology and distribution of carbon

https://doi.org/10.1021/acsomega.4c07009
ACS Omega 2024, 9, 39259–39276

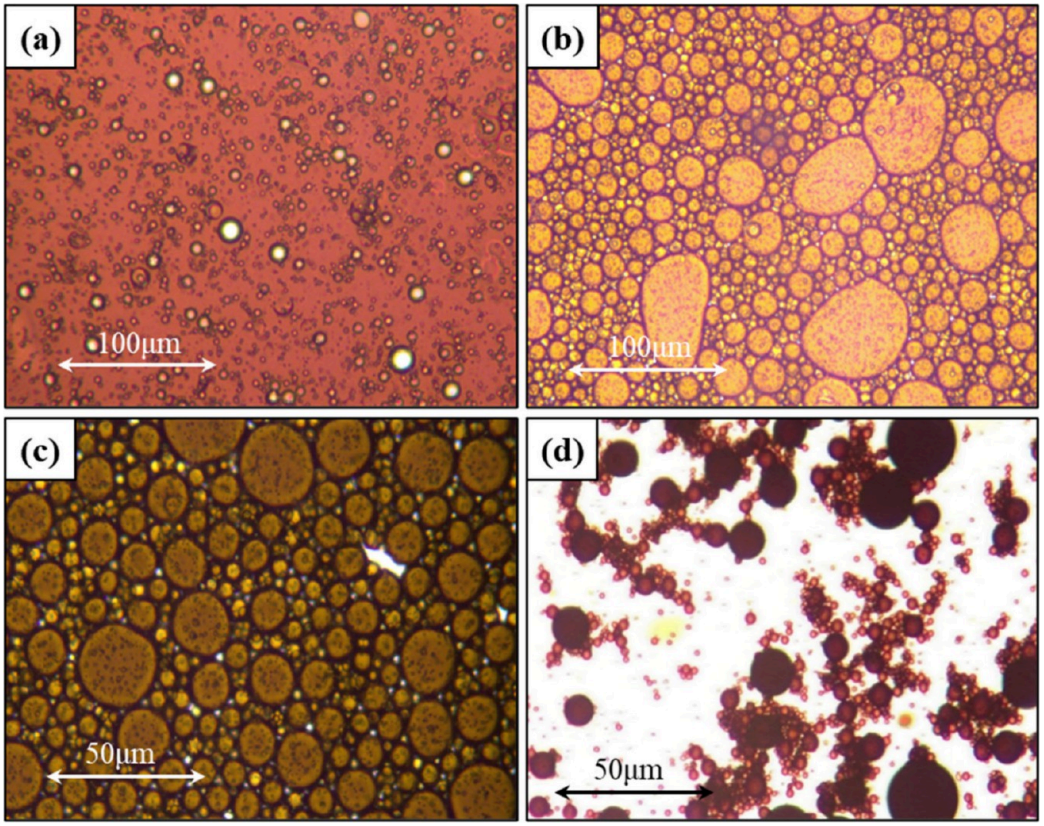

Figure 19. Morphology of emulsions. (a) Water droplet at oil−water ratio 9:1; (b) oil droplet at 1% compounding system (NaOl: CAB-35 = 1:2); (c) oil droplet at 1% compounding system and 0.1% alkalis (TEOA:NaOH = 1:1); (d) oil droplet 1% compounding system, 0.1% alkalis, and 0.2 mol/L inorganic salt.

atoms are presented for both crude and emulsion samples. Figure. 21a illustrates that crude exhibits a high wetting morphology on steel for filling the surface scratching traces. Upon the addition of surfactants, the wetting behavior of the emulsion on the metal surface diminishes, resulting in a clearer outline of the emulsion droplets in Figure 21b. This observation is further corroborated by the surface scanning of the carbon atomic distribution shown in Figure 21c and Figure 21d, indicating a shift in wettability due to the substitution of oil with the surfactant solution. The shift in wettability is caused by the adsorption of the long alkyl chain lipophilic groups on surfactant molecules at the oil−water interface. The polar hydrophilic groups extend to the interface, forming hydrogen bonds with water molecules and creating a water film that alters the wettability of the pipe.[63] This alteration in wettability ultimately leads to a reduction in the flow resistance of emulsions during subsequent transportation.

3.3.4. Synergistic Mechanism of Anionic and Zwitterionic Surfactants. The electrostatic potentials of surfactants and asphaltene are visualized in red, white, and blue, as depicted in Figure 22. The red region indicates a positive charge where atoms have difficulty losing electrons, but atoms can easily receive electrons to form hydrogen bonds. Conversely, the blue region represents a negative charge where atoms are more likely to lose electrons. The white region has a near-zero potential and exhibits a relatively stable structure. Specifically, in the NaOl molecule, significant positive and negative charges gather near the carboxyl substituent and Na atom (Figure 22a). Similarly, in the CAB-35 molecule, a substantial accumulation of charges is observed around the N atom and carboxyl substituent (Figure 22b). In asphaltene, this phenomenon is prominent near N atoms and hydroxyl groups (Figure 22c).

As illustrated in Figure 23, the amorphous cells (AC) for both the oil phase and the solution phase have been established. The oil phase contains 10 asphaltene molecules, while the solution phase comprises 5 NaOl molecules, 10 CAB-35 molecules, 2 TEOA molecules, 2 NaOH molecules, and 600 water molecules. Additionally, a single surfactant solution AC is also prepared, consisting of 600 water molecules and either 10 NaOl or 10 CAB-35 molecules. Following the optimization process detailed in Section 2.3.5, the phase interface is constructed using the Build Layer function. A vacuum layer of 20 Å is introduced between the interfaces, after which the Forcite module facilitates a 500 ps molecular dynamics simulation.

3.3.4.1. Interaction Energy. The interaction strength of each component in the emulsion can be characterized by the interaction energy (E_{int}). The lower the E_{int} indicates the stronger interaction of components and the stabler structure.[64] E_{int} and Nonbond energy (E_{non}) are calculated using the COMPASS III force field of Forcite module as eq 10 and eq 11. The comparison of system energy is shown in Table 5.

$$E_{int} = E_{A\text{-}B} - (E_A + E_B) \tag{10}$$

$$E_{non} = E_{dvW} + E_{elec} \tag{11}$$

where E_{int}, $E_{A\text{-}B}$, E_A, and E_B are the energy of interaction, the system total energy and the energy of each component, kcal/mol; E_{non}, E_{dvW}, and E_{elec} are the Nonbond energy, van der

https://doi.org/10.1021/acsomega.4c07009
ACS Omega 2024, 9, 39259−39276

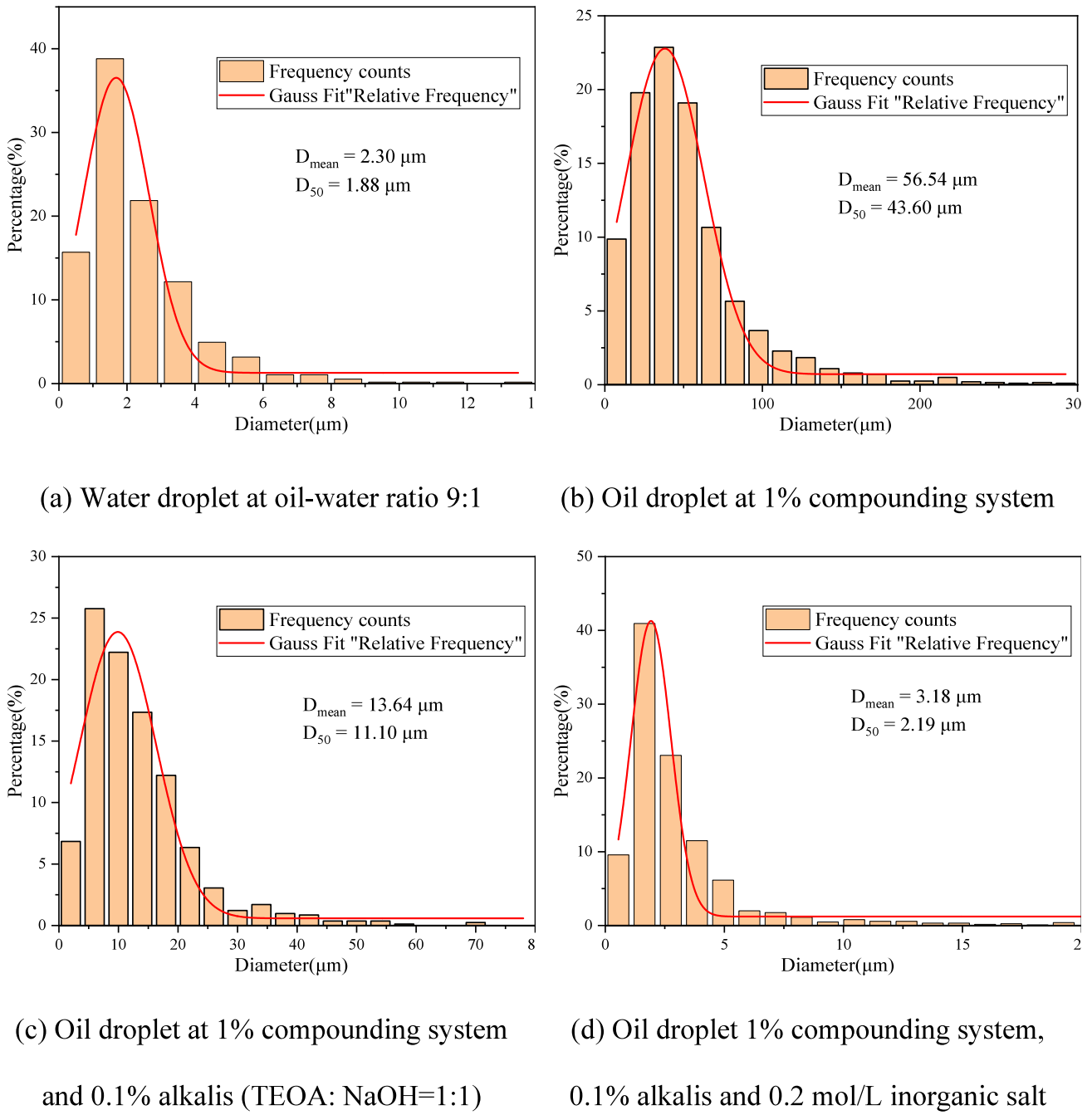

(a) Water droplet at oil-water ratio 9:1

(b) Oil droplet at 1% compounding system

(c) Oil droplet at 1% compounding system and 0.1% alkalis (TEOA: NaOH=1:1)

(d) Oil droplet 1% compounding system, 0.1% alkalis and 0.2 mol/L inorganic salt

Figure 20. Droplet size distribution of emulsions.

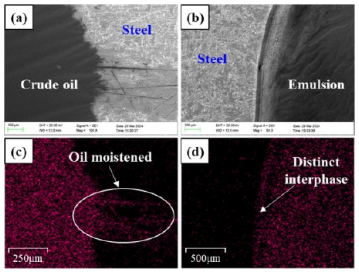

Figure 21. SEM and EDS images of crude and emulsion: (a) crude SEM; (b) emulsion SEM; (c) carbon atom EDS of crude; (d) carbon atom EDS of emulsion.

Waals interaction energy and the electrostatic interaction energy, kcal/mol.

As shown in Table 5, the results of E_{int} and E_{non} are equal, indicating the adsorption of surfactants and asphaltene in the heavy oil emulsification.[65] Under alkaline conditions, the interaction between CAB-35 and NaOL is enhanced, resulting in a decrease in the E_{int}. It is observed that a single surfactant can achieve a negative E_{int} with asphaltene. Furthermore, the combination of surfactants with asphaltene results in a lower E_{int} compared with using either agent individually. Importantly, the proportion of E_{elec} in E_{non} consistently surpasses that of E_{vdW} in all of the systems. Hence, the viscosity reduction in emulsification is primarily attributed to the strong electrostatic

https://doi.org/10.1021/acsomega.4c07009
ACS Omega 2024, 9, 39259−39276

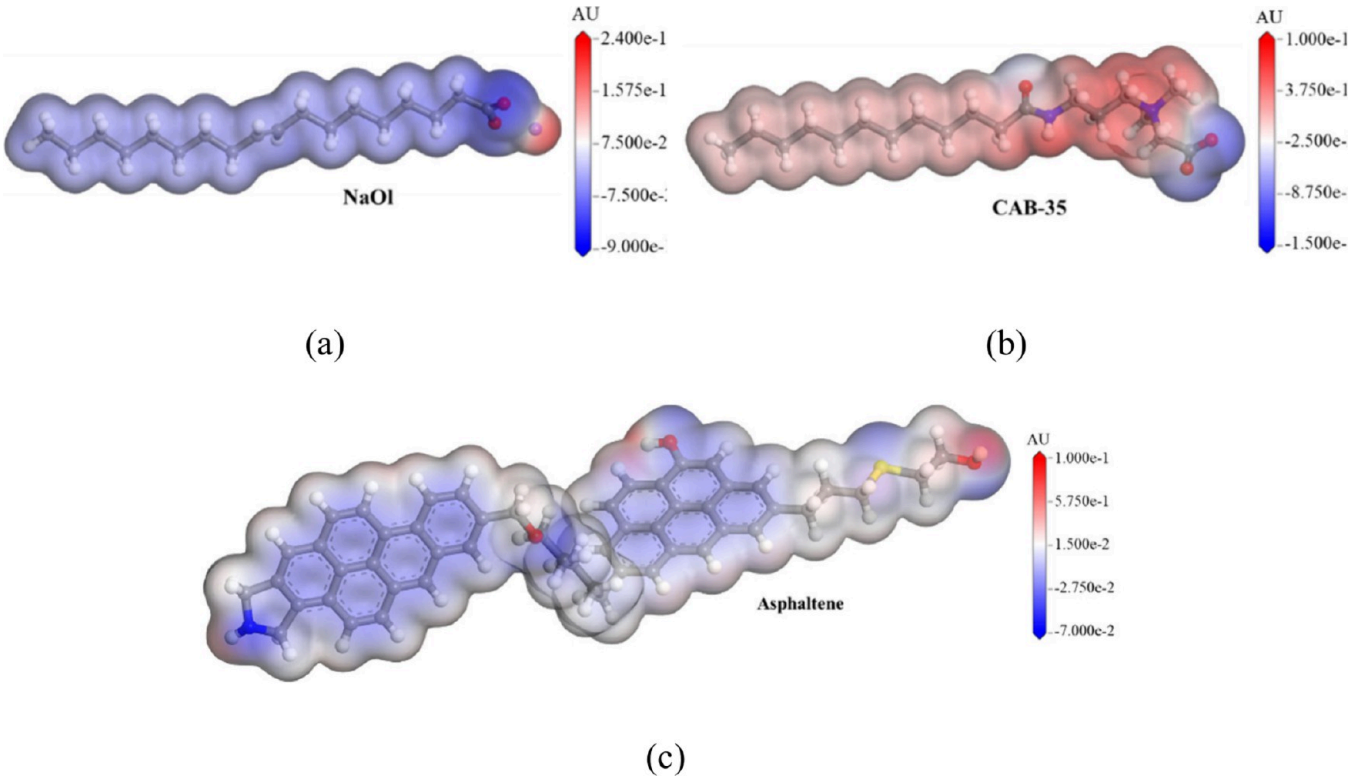

Figure 22. Electrostatic potential of surfactants and asphaltene.

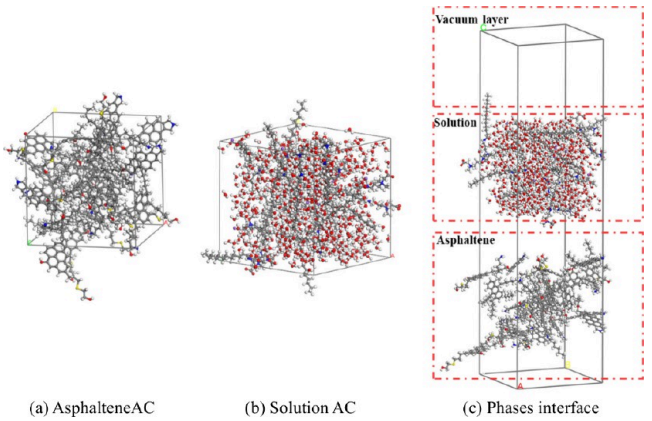

Figure 23. Amorphous cells and phase interface.

interaction arising from molecular electrostatic potential distributions.

3.3.4.2. Radial Distribution Function (RDF). Figure 24a illustrates the radial distribution function (RDF) curve for oxygen atoms in asphaltene and hydrogen atoms in water molecules during the emulsification process. The curve reveals two sharp peaks within the range of 1−4 Å. The alignment of the peak positions suggests that the aggregation structures of asphaltene and the solution molecules are similar within this range. Notably, the peak sizes indicate that asphaltene exhibits stronger interactions with water molecules and Na^+ ions in NaOl solution compared to those in CAB-35 solution (Figure 24b). Furthermore, the peaks associated with NaOl, CAB-35, and alkali molecules are higher, signifying an enhanced interaction.

3.3.4.3. Hydrogen-Bond Interaction. Figure 25 illustrates the changes in hydrogen bonds within the emulsion system, as calculated by the script. The criteria for identifying hydrogen bonds in the script stipulate that the donor−acceptor distance must be less than 3 Å, and the angle between the hydrogen atom-donor−acceptor is less than 30°. Initially, there are no hydrogen bonds present between the two phases due to the lack of contact. Approximately 60 ps into the simulation, the oil and water phases make contact, allowing the polar headgroup of the surfactant to form hydrogen bonds with water molecules. It rapidly establishes a new oil−water interface. Subsequently, the number of hydrogen bonds quickly increases at the expanded interface. And the surfactant molecules continue to diffuse due to hydrophobic interactions,

Table 5. Comparison of Surfactant/Asphaltene System Energy

System	System energy (kcal/mol)						
	E_{non}	E_{vdW}	E_{elec}	E_{int}	$E_{A\text{-}B}$	E_A	E_B
CAB-35/NaOL	12.97	−0.58	13.55	12.97	−299.71	−120.27	−192.41
CAB-35/NaOL (Alkali)	2.68	0.05	2.63	2.68	−269.80	−101.05	−171.42
NaOL/Asphaltene	−4.25	−0.07	−4.18	−4.25	611.45	807.60	−191.89
CAB-35/Asphaltene	−15.28	−0.02	−15.26	−15.28	736.33	805.51	−53.89
CAB-35+NaOL/Asphaltene (Alkali)	−16.52	−0.60	−15.92	−16.52	515.04	812.61	−281.04

https://doi.org/10.1021/acsomega.4c07009
ACS Omega 2024, 9, 39259−39276

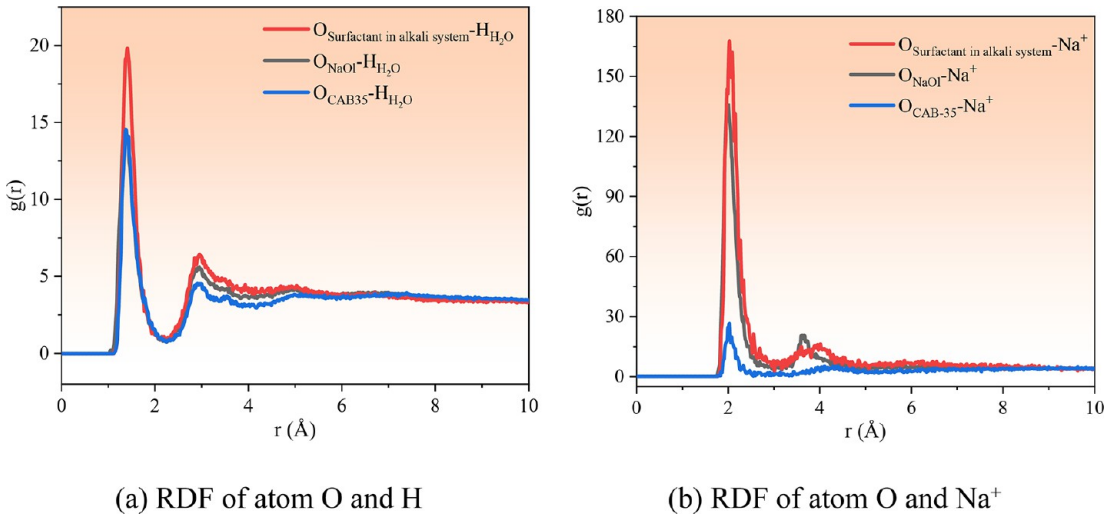

(a) RDF of atom O and H (b) RDF of atom O and Na^+

Figure 24. RDF between atoms in different surfactant systems.

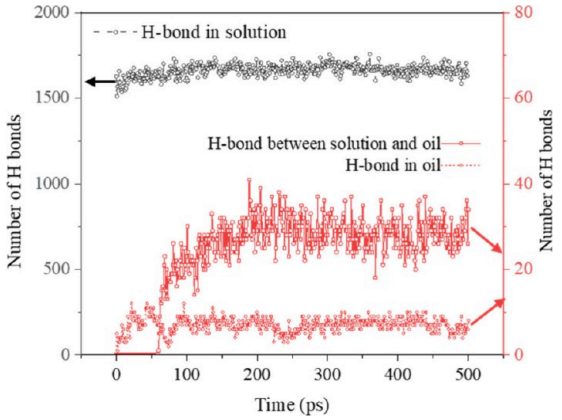

Figure 25. Internal and interphase hydrogen bonding.

leading to a gradual stabilization of the hydrogen bond distribution.[66]

3.3.4.4. Synergistic Mechanism. The synergistic effect of the emulsification viscosity reduction mechanism of anionic and zwitterionic surfactants is shown in Figure 26. The introduction of surfactants effectively reduced the oil−water interfacial tension. Concurrently, the long alkyl chain lipophilic groups of the surfactant molecules adsorb at the oil−water interface. The polar hydrophilic groups extend and interact with water molecules through hydrogen bonds to form a water film that facilitates emulsification and reduces the viscosity. Under alkaline conditions, when NaOl and CAB-35 diffuse to the oil−water interface, the − OH in asphaltene and resin connect NaOl through hydrogen bonds[67] and water bridge.[68] The asphaltenes in the heavy oil partially replace with the surfactant, resulting in the formation of an O/W emulsion[69] and exhibiting shear thinning behavior.[70]

4. CONCLUSIONS

This study investigates the effects of a compounding surfactant system consisting of anionic NaOl and zwitterionic CAB-35 on the South China Sea heavy oil. The aim is to understand the

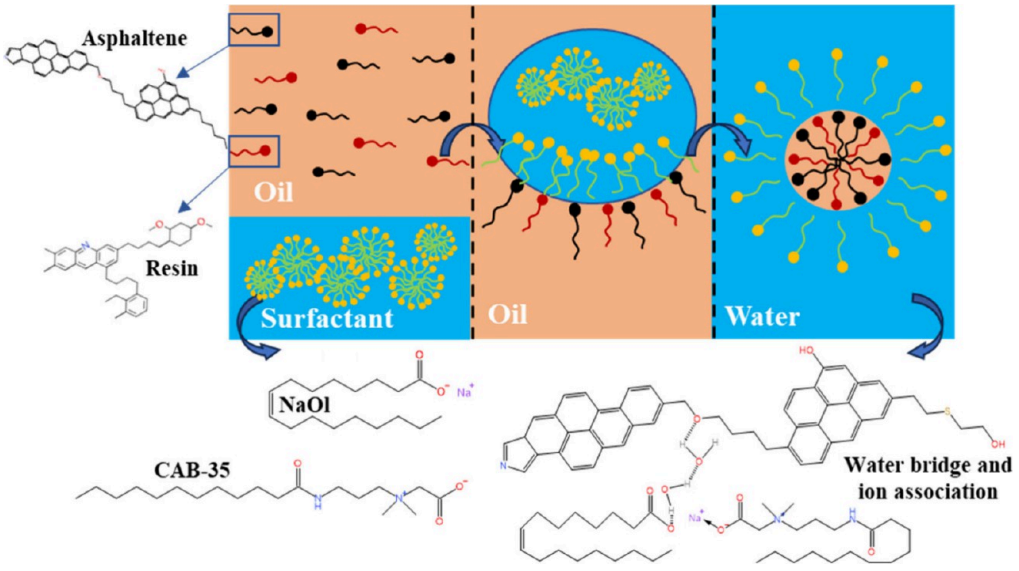

Figure 26. Synergistic mechanism of the anionic and zwitterionic surfactants.

https://doi.org/10.1021/acsomega.4c07009
ACS Omega 2024, 9, 39259−39276

impact of emulsification conditions and the viscosity reduction mechanism.

The most effective viscosity reduction solution consists of a combination of 1% NaOl and CAB-35 in a mass ratio of 1:2, along with the addition of 0.1% NaOH and TEOA in a mass ratio of 1:1. This solution maintains an oil−water ratio of 7:3, with emulsification occurring at a temperature of 30 °C and a stirring rate of 1000 rpm. The surfactant system demonstrated a significant viscosity reduction effect, achieving a viscosity reduction rate of 94.95%. The interfacial tension significantly reduced from 27 to 4 mN/m and transformed the oil droplet being rounder and smaller. The increase in salinity promotes flocculation between the surfactant and asphaltenes/colloids. The emulsion viscosity increases slightly at the salinity of 0.2 mol/L and the D_{mean} size is measuring as 3 μm. Surfactant molecules with long alkyl chain lipophilic groups adsorb at the oil−water interface, while the polar hydrophilic groups extend to form hydrogen bonds with water molecules, creating a water film. This alteration in steel surface wettability shifts it from being oil-wet to being water-wet, ultimately reducing the drag. The viscosity reduction in the emulsification is primarily attributed to the strong electrostatic interaction arising from molecular electrostatic potential distributions. The −OH in asphaltene and resin molecules connects the surfactant molecule through hydrogen bonds and a water bridge, resulting in the formation of a shear dilution of the O/W emulsion.

In summary, the results of this study offer insights for viscosity control. Since the research is conducted under specific experimental conditions, it is essential to conduct additional oil field experiments focusing on long-term storage and transportation. The conditions for maximizing of the synergistic mechanism warrant further investigation.

AUTHOR INFORMATION

Corresponding Author

Yuting Shan − *School of Oil & Natural Gas Engineering, Southwest Petroleum University, Chengdu 610500, China;* orcid.org/0000-0002-3895-5908; Email: shanyt12138@163.com

Authors

Jiaqiang Jing − *School of Oil & Natural Gas Engineering, Southwest Petroleum University, Chengdu 610500, China; Oil & Gas Fire Protection Key Laboratory of Sichuan Province, Chengdu 610500, China;* orcid.org/0000-0003-4219-0829

Ning Wang − *School of Oil & Natural Gas Engineering, Southwest Petroleum University, Chengdu 610500, China*

Jie Sun − *School of Oil & Natural Gas Engineering, Southwest Petroleum University, Chengdu 610500, China; Oil & Gas Fire Protection Key Laboratory of Sichuan Province, Chengdu 610500, China*

Cancan Jiang − *School of Oil & Natural Gas Engineering, Southwest Petroleum University, Chengdu 610500, China*

Lei Cao − *School of Oil & Natural Gas Engineering, Southwest Petroleum University, Chengdu 610500, China*

Xiyuan Song − *School of New Energy and Materials, Southwest Petroleum University, Chengdu 610500, China*

Complete contact information is available at: https://pubs.acs.org/10.1021/acsomega.4c07009

Notes

The authors declare no competing financial interest.

ACKNOWLEDGMENTS

This work is supported by the National Natural Science Foundation of China (Grant No. 52106208) and Natural Science Foundation of Sichuan Province (Grant No. 2023NSFSC0924).

REFERENCES

(1) Zamora Garcia Rojas, D.; Gallardo Rivas, N. V.; Mendoza de la Cruz, J. L.; Salazar Cruz, B. A.; Paramo Garcia, U. Effect of non-ionic surfactants on the transport properties of an emulsified heavy oil. *Fuel* **2021**, *300*, 120934.

(2) Saad, M. A.; Kamil, M.; Abdurahman, N. H.; Yunus, R. M.; Awad, O. I. An Overview of Recent Advances in State-of-the-Art Techniques in the Demulsification of Crude Oil Emulsions. *Processes* **2019**, *7* (7), 470.

(3) Yanuar; Gunawan; Setiawan, M. R.; Febriansyah, W.; Arianda, A. Drag Reduction by Surfactant of Crude Oil Flow in Pentagon Spiral Pipe. In *4th International Tropical Renewable Energy Conference (i-TREC) - Sustainable Energy and Environment for Tropical Climate*; Bali, Indonesia, Aug 14−16, 2019 ; AIP Publishing, 2019.

(4) Yang, Z.; Ma, G.; Hu, Z. Mechanism of the viscosity reduction with ternary compound in the sulfonate-straight chain alcohol-alkaline compound system. *Petroleum Science and Technology* **2019**, *37* (1), 1−7.

(5) Sharma, R.; Deka, B.; Mandal, A.; Mahto, V. Study the influence of sodium dodecyl sulfate on emulsification of heavy and waxy crude oils to improve their flow ability in low temperature conditions. *Asia-Pacific Journal of Chemical Engineering* **2019**, *14* (1), e2279.

(6) Pu, W. F.; Shen, C.; Tang, X. J.; Pang, S. S.; Sun, D.; Mei, Z. L. Emulsification of acidic heavy oil for viscosity reduction and enhanced oil recovery. *J. Dispersion Sci. Technol.* **2020**, *41* (1), 54−61.

(7) Li, J.; Wang, Q. X.; Liu, Y. G.; Wang, M. G.; Tan, Y. B. Long Branched-Chain Amphiphilic Copolymers: Synthesis, Properties, and Application in Heavy Oil Recovery. *Energy Fuels* **2018**, *32* (6), 7002−7010.

(8) Khidr, T. T.; Ahmed, S. M. The effect of cationic surfactant additives on flow properties of crude oil. *Petroleum Science and Technology* **2016**, *34* (14), 1219−1225.

(9) Massarweh, O.; Abushaikha, A. S. The synergistic effects of cationic surfactant and smart seawater on the recovery of medium-viscosity crude oil from low-permeability carbonates. *J. Mol. Liq.* **2023**, *389*, 122866.

(10) Koreh, P.; Lashkarbolooki, M.; Peyravi, M.; Jahanshahi, M. Interfacial performance of cationic, anionic and non-ionic surfactants; effect of different characteristics of crude oil. *J. Pet. Sci. Eng.* **2022**, *218*, 110960.

(11) Marhaendrajana, T.; Kurnia, R.; Irfana, D.; Abdassah, D.; Wahyuningrum, D. Study to improve an amphoteric sulfonate alkyl ester surfactant by mixing with nonionic surfactant to reduce brine-waxy oil interfacial tension and to increase oil recovery in sandstone reservoir: T-KS field, Indonesia. *Journal of Petroleum Exploration and Production Technology* **2019**, *9* (1), 675−683.

(12) Ma, H.; Ranimol, S.; Cameron, A. Synergetic System of Zwitterionic/Anionic Surfactants with Ultralow Interfacial Tension and High Salt Resistance for Enhancing Heavy Oil Recovery. *Energy Fuels* **2022**, *36* (15), 8216−8223.

(13) Lu, H. S.; Guan, X. Q.; Wang, B. G.; Huang, Z. Y. CO2-Switchable Oil/Water Emulsion for Pipeline Transport of Heavy Oil. *J. Surfactants Deterg.* **2015**, *18* (5), 773−782.

(14) Yang, Z.; Ma, G.; Hu, Z.; Zhai, W. Characterization of ternary compound viscosity reducer system on viscosity of viscous crude oil. *Petroleum Science and Technology* **2017**, *35* (19), 1910−1916.

(15) Liu, M.; Wu, Y.; Zhang, L.; Rong, F.; Yang, Z. Mechanism of viscosity reduction in viscous crude oil with polyoxyethylene

https://doi.org/10.1021/acsomega.4c07009
ACS Omega 2024, 9, 39259−39276

surfactant compound system. *Petroleum Science and Technology* **2019**, *37* (4), 409−416.
(16) Kumar, R.; Bora, G. S.; Banerjee, S.; Mandal, A.; Naiya, T. K. Application of naturally extracted surfactant from Madhuca longifolia to improve the flow properties of heavy crude oil through horizontal pipeline. *J. Pet. Sci. Eng.* **2018**, *168*, 178−189.
(17) Mandal, A.; Kar, S.; Kumar, S. The Synergistic Effect of a Mixed Surfactant (Tween 80 and SDBS) on Wettability Alteration of the Oil Wet Quartz Surface. *J. Dispersion Sci. Technol.* **2016**, *37* (9), 1268−1276.
(18) Ma, H.; Ranimol, S.; Cameron, A. Synergetic System of Zwitterionic/Anionic Surfactants with Ultralow Interfacial Tension and High Salt Resistance for Enhancing Heavy Oil Recovery. *Energy & Fuels* **2022**, *36*, 8216.
(19) Si, Y. W.; Zhu, Y. W.; Liu, T.; Xu, X. R.; Yang, J. Y. Synthesis of a novel borate ester Anion-Nonionic surfactant and its application in viscosity reduction and emulsification of heavy crude oil. *Fuel* **2023**, *333*, 126453.
(20) Wang, J.; Liu, R.; Tang, Y.; Zhu, J.; Sun, Y.; Zhang, G. *Synthesis of Polycarboxylate Viscosity Reducer and the Effect of Different Chain Lengths of Polyether on Viscosity Reduction of Heavy Oil* **2022**, *14* (16), 3367.
(21) Wang, J.; Liu, R.; Wang, B.; Cheng, Z.; Liu, C.; Tang, Y.; Zhu, J. Synthesis of Polyether Carboxylate and the Effect of Different Electrical Properties on Its Viscosity Reduction and Emulsification of Heavy Oil. *Polymers [Online]* **2023**, *15*, 3139.
(22) Wenqi, Z.; Guiyang, M.; Zhiyong, H. Effect of organic alkali, n-alkanol, and nonionic surfactant ternary compound system on viscosity reduction of viscous crude oil. *Petroleum Science and Technology* **2019**, *37* (9), 989−996.
(23) Zhang, H. Y.; Dong, M. Z.; Zhao, S. Q. Experimental Study of the Interaction between NaOH, Surfactant, and Polymer in Reducing Court Heavy Oil/Brine Interfacial Tension. *Energy Fuels* **2012**, *26* (6), 3644−3650.
(24) Noruzi, Y.; Sharifi, M.; Fahimpour, J.; Sabet, M.; Akbari, M.; Hosseini, S. The State-of-the-Art of wettability alteration in sandstones and Carbonates: A mechanistic review. *Fuel* **2024**, *356*, 129570.
(25) Zhang, F. F.; Liu, Y. G.; Wang, Q. X.; Han, Y. G.; Yan, Z. H.; Chen, H.; Tan, Y. B. Fabricating a heavy oil viscosity reducer with weak interaction effect: Synthesis and viscosity reduction mechanism. *Colloid and Interface Science Communications* **2021**, *42*, 100426.
(26) Gao, Y.; Wu, B.; Gao, J.; Wang, L.; Zhao, W.; Gui, Z. The Formation of Waxy Crude Oil-in-water Emulsions for the Reduction of Pour Point and Viscosity. *Petroleum Science and Technology* **2013**, *31* (23), 2443−2450.
(27) Liu, J. B.; Zhong, L. G.; Hao, T. C.; Ren, L.; Liu, Y. G. A collaborative emulsification system capable of forming stable small droplets of oil-in-water emulsions for enhancing heavy oil recovery. *J. Mol. Liq.* **2022**, *355*, 118970.
(28) Vegad, G. D.; Jana, A. K. Viscosity Reduction of Indian Heavy Crude Oil by Emulsification to O/W Emulsion Using Polysorbate-81. *J. Surfactants Deterg.* **2021**, *24* (2), 301−311.
(29) Abdurahman, N. H.; Rosli, Y. M.; Azhari, N. H.; Hayder, B. A. Pipeline transportation of viscous crudes as concentrated oil-in-water emulsions. *J. Pet. Sci. Eng.* **2012**, *90*−*91*, 139−144.
(30) Kumar, S.; Mahto, V. Emulsification of Indian heavy crude oil in water for its efficient transportation through offshore pipelines. *Chemical Engineering Research & Design* **2016**, *115*, 34−43.
(31) Pu, W. F.; Shen, C.; Pang, S. S.; Tang, X. J.; Chen, B. W.; Mei, Z. L. Viscosity reduction of acidic heavy oil through emulsification: effects of salinity and pH. *Petroleum Science and Technology* **2019**, *37* (4), 402−408.
(32) Zhang, X.; Guo, J.; Gao, C.; Kiyingi, W.; Wang, L.; Fei, D.; Peng, Z.; Li, J.; Dong, J. A molecular study of viscosity-causing mechanism and viscosity reduction through re-emulsification for Jimsar shale oil. *J. Mol. Liq.* **2023**, *392*, No. 123470.
(33) Cai, H.-Y.; Zhang, Y.; Liu, Z.-Y.; Li, J.-G.; Gong, Q.-T.; Liao, Q.; Zhang, L.; Zhao, S. Molecular dynamics simulation of binary betaine and anionic surfactant mixtures at decane - Water interface. *J. Mol. Liq.* **2018**, *266*, 82−89.
(34) Zhang, F.; Liu, Y.; Wang, Q.; Han, Y.; Yan, Z.; Chen, H.; Tan, Y. Fabricating a heavy oil viscosity reducer with weak interaction effect: Synthesis and viscosity reduction mechanism. *Colloid and Interface Science Communications* **2021**, *42*, No. 100426.
(35) Wang, C.; Zhong, L.; Cao, Z.; Liu, Y.; Zou, J.; Wang, Q. Synergistic Collaboration between a Viscosity Reducer and a Surfactant for in Situ Emulsion Formation to Enhance Heavy-Oil Recovery. *Energy Fuels* **2020**, *34* (1), 95−102.
(36) Jia, H.; Song, J. Y.; Sun, Y. Q.; Xu, M. M.; Li, C. Q.; Wei, Z. W.; Cao, W. X.; Wang, X. Y.; Lv, K. H.; Liu, D. X. Novel Molecular Insights into the Effects of Ethoxy Group Number on Emulsification and Viscosity Reduction of Anionic-Nonionic Surfactants. *Energy Fuels* **2023**, *37* (20), 15615−15625.
(37) Schulz, E. N.; Ambrusi, R. E.; Miraglia, D. B.; Schulz, E. P.; García, S. G.; Rodriguez, J. L.; Schulz, P. C. Evaluation of oil-in-water emulsions with cationic-anionic surfactants mixtures for potential use in the oil industry. *Colloids and Surfaces a-Physicochemical and Engineering Aspects* **2016**, *490*, 145−154.
(38) Waglewska, E.; Bazylinska, U. Biodegradable Amphoteric Surfactants in Titration-Ultrasound Formulation of Oil-in-Water Nanoemulsions: Rational Design, Development, and Kinetic Stability. *International Journal of Molecular Sciences* **2021**, *22* (21), 11776.
(39) Zhang, F.; Zhang, Q.; Zhou, Z. H.; Sun, L. L.; Zhou, Y. W. Study on the Effect of Different Viscosity Reducers on Viscosity Reduction and Emulsification with Daqing Crude Oil. *Molecules* **2023**, *28* (3), 1399.
(40) Shibaev, A. V.; Kuklin, A. I.; Philippova, O. E. Different responsiveness to hydrocarbons of linear and branched anionic/cationic-mixed wormlike surfactant micelles. *Colloid Polym. Sci.* **2019**, *297* (3), 351−362.
(41) Wu, R. A.; Yan, Y. H.; Li, X. X.; Tan, Y. B. Preparation and controllable heavy oil viscosity reduction performance of pH-responsive star block copolymers. *J. Mol. Liq.* **2023**, *389*, 122925.
(42) Wang, K. L.; Zhang, B. W.; Li, G. Effects of weak-alkali ASP composition on the stability of O/W emulsions. *Energy Sources Part a-Recovery Utilization and Environmental Effects* **2019**, *41* (4), 438−450.
(43) Wen, J. B.; Zhang, J. J.; Wei, M. Effective viscosity prediction of crude oil-water mixtures with high water fraction. *J. Pet. Sci. Eng.* **2016**, *147*, 760−770.
(44) Yu, L.; Li, S. D.; Stubbs, L. P.; Lau, H. C. Characterization of clay-stabilized, oil-in-water Pickering emulsion for potential conformance control in high-salinity, high-temperature reservoirs. *Appl. Clay Sci.* **2021**, *213*, 106246.
(45) Sumitomo, S.; Ueta, M.; Uddin, M. A.; Kato, Y. Comparison of Oil-in-Water Emulsion between Ultrasonic Irradiation and Mechanical Stirring. *Chem. Eng. Technol.* **2019**, *42* (2), 381−387.
(46) Moribe, H.; Kitayama, Y.; Suzuki, T.; Okubo, M. Emulsifier-Free, Organotellurium-Mediated Living Radical Emulsion Polymerization of Styrene: Effect of Stirring Rate. *Macromolecules* **2011**, *44* (2), 263−268.
(47) Nanikashvili, P. M.; Butenko, A. V.; Deutsch, M.; Lee, D. Y.; Sloutskin, E. Salt-induced stability and modified interfacial energetics in self-faceting emulsion droplets. *J. Colloid Interface Sci.* **2022**, *621*, 131−138.
(48) Sun, N. N.; Jing, J. Q.; Jiang, H. Y.; An, Y. P.; Wu, C.; Zheng, S. J.; Qi, H. Y. Effects of Surfactants and. Alkalis on the Stability of Heavy-Oil-in-Water Emulsions. *Spe Journal* **2017**, *22* (1), 120−129.
(49) Kundu, P.; Agrawal, A.; Mateen, H.; Mishra, I. M. Stability of oil-in-water macro-emulsion with anionic surfactant: Effect of electrolytes and temperature. *Chem. Eng. Sci.* **2013**, *102*, 176−185.
(50) Zhai, X. G.; Gao, J. P.; Wang, X. X.; Mei, S. K.; Zhao, R. R.; Wu, Y. L.; Hao, C. Y.; Yang, J. B.; Liu, Y. Inverse Pickering emulsions stabilized by carbon quantum dots: Influencing factors and their application as templates. *Chemical Engineering Journal* **2018**, *345*, 209−220.
(51) Saberi, A. H.; Fang, Y.; McClements, D. J. Effect of Salts on Formation and Stability of Vitamin E-Enriched Mini-emulsions

https://doi.org/10.1021/acsomega.4c07009
ACS Omega 2024, 9, 39259−39276

Produced by Spontaneous Emulsification. *J. Agric. Food Chem.* **2014**, *62* (46), 11246−11253.
(52) Nie, C. H.; Han, G. Q.; Ni, J. W.; Guan, S. X.; Du, H.; Zhang, Y. P.; Wang, H. T. Stability Dynamic Characteristic of Oil-in-Water Emulsion from Alkali-Surfactant-Polymer Flooding. *Acs Omega* **2021**, *6* (29), 19058−19066.
(53) Zhu, D.; Li, B. F.; Li, H. F.; Li, B. L.; Cao, Y. B.; Li, Z. M. Effects of low-salinity water on the interface characteristics and imbibition process. *J. Pet. Sci. Eng.* **2022**, *208*, 109564.
(54) Kumar, S.; Mandal, A. Studies on interfacial behavior and wettability change phenomena by ionic and nonionic surfactants in presence of alkalis and salt for enhanced oil recovery. *Appl. Surf. Sci.* **2016**, *372*, 42−51.
(55) Gürses, A.; Karaca, S.; Açikyildiz, M.; Ejder, M. Thermodynamics and mechanism of cetyltrimethylammonium adsorption onto clayey soil from aqueous solutions. *Chemical Engineering Journal* **2009**, *147* (2−3), 194−201.
(56) Luo, H. J.; Wen, J. B.; Jiang, R.; Shao, Q. Q.; Wang, Z. H. Modeling of the Phase Inversion Point of Crude Oil Emulsion by Characterization of Crude Oil Physical Properties. *Acs Omega* **2022**, *7*, 39136.
(57) Munoz-Ibanez, M.; Azagoh, C.; Dubey, B. N.; Dumoulin, E.; Turchiuli, C. Changes in oil-in-water emulsion size distribution during the atomization step in spray-drying encapsulation. *Journal of Food Engineering* **2015**, *167*, 122−132.
(58) dos Santos, R. G.; Bannwart, A. C.; Briceño, M. I.; Loh, W. Physico-chemical properties of heavy crude oil-in-water emulsions stabilized by mixtures of ionic and non-ionic ethoxylated nonylphenol surfactants and medium chain alcohols. *Chemical Engineering Research & Design* **2011**, *89* (7A), 957−967.
(59) Chanamai; Herrmann; McClements. Ultrasonic Spectroscopy Study of Flocculation and Shear-Induced Floc Disruption in Oil-in-Water Emulsions. *J. Colloid Interface Sci.* **1998**, *204* (2), 268−76.
(60) Delahaije, R.; Hilgers, R. J.; Wierenga, P. A.; Gruppen, H. Relative contributions of charge and surface coverage on pH-induced flocculation of protein-stabilized emulsions. *Colloids and Surfaces a-Physicochemical and Engineering Aspects* **2017**, *521*, 153−160.
(61) Santos, J.; Calero, N.; Trujillo-Cayado, L. A.; Alfaro, M. C.; Muñoz, J. The Role of Processing Temperature in Flocculated Emulsions. *Ind. Eng. Chem. Res.* **2018**, *57* (3), 807−812.
(62) Ahmad, A. L.; Kusumastuti, A.; Derek, C. J. C.; Ooi, B. S. Emulsion liquid membrane for heavy metal removal: An overview on emulsion stabilization and destabilization. *Chemical Engineering Journal* **2011**, *171* (3), 870−882.
(63) Li, L.; Liu, Z. The role of the interface on surfactant transport to crude oil-water liquid-liquid interface. *J. Mol. Liq.* **2024**, *395*, No. 123849.
(64) Zhang, J. X.; Yang, C.; Niu, F. S.; Gao, S. L. Molecular dynamics study on selective flotation of hematite with sodium oleate collector and starch-acrylamide flocculant. *Appl. Surf. Sci.* **2022**, *592*, 153208.
(65) Yuan, M. Y.; Nie, W.; Yu, H.; Yan, J. Y.; Bao, Q.; Zhou, W. W.; Hua, Y.; Guo, L. D.; Niu, W. J. Experimental and molecular dynamics simulation study of the effect of different surfactants on the wettability of low-rank coal. *Journal of Environmental Chemical Engineering* **2021**, *9* (5), 105986.
(66) Li, L.; Liu, Z. The role of the interface on surfactant transport to crude oil-water liquid-liquid interface. *J. Mol. Liq.* **2024**, *395*, 123849.
(67) Sierra, M. B.; Morini, M. A.; Schulz, P. C.; Junquera, E.; Aicart, E. Effect of Double Bonds in the Formation of Sodium Dodecanoate and Sodium 10-Undecenoate Mixed Micelles in Water. *J. Phys. Chem. B* **2007**, *111* (40), 11692−11699.
(68) Messina, P.; Morini, M. A.; Schulz, P. C. Aqueous sodium oleate−sodium dehydrocholate mixtures at low concentration. *Colloid Polym. Sci.* **2003**, *281* (11), 1082−1091.
(69) Liu, D.; Li, C.; Yang, F.; Sun, G.; You, J.; Cui, K. Synergetic effect of resins and asphaltenes on water/oil interfacial properties and emulsion stability. *Fuel* **2019**, *252*, 581−588.
(70) dos Santos, R. G.; Bannwart, A. C.; Loh, W. Phase segregation, shear thinning and rheological behavior of crude oil-in-water emulsions. *Chem. Eng. Res. Des.* **2014**, *92* (9), 1629−1636.

https://doi.org/10.1021/acsomega.4c07009
ACS Omega 2024, 9, 39259−39276